

Transport through constricted quantum Hall edge systems: Beyond the quantum point contact

Siddhartha Lal*

The Abdus Salam ICTP, Strada Costiera 11, Trieste 34014, Italy

(Received 20 September 2007; published 29 January 2008)

Motivated by surprises in recent experimental findings, we study transport in a model of a quantum Hall edge system with a gate-voltage controlled constriction. A finite backscattered current at finite edge bias is explained from a Landauer-Buttiker analysis as arising from the splitting of edge current caused by the difference in the filling fractions of the bulk (ν_1) and constriction (ν_2) quantum Hall fluid regions. We develop a hydrodynamic theory for bosonic edge modes inspired by this model. The constriction region splits the incident long-wavelength chiral edge density-wave excitations among the transmitting and reflecting edge states encircling it. The competition between two interedge tunneling processes taking place inside the constriction, related by a quasiparticle-quasihole (qp-qh) symmetry, is accounted for by computing the boundary theories of the system. This competition is found to determine the strong coupling configuration of the system. A separatrix of qp-qh symmetric gapless critical states is found to lie between the relevant renormalization group (RG) flows to a metallic and an insulating configuration of the constriction system. This constitutes an interesting generalization of the Kane-Fisher quantum impurity model. The features of the RG phase diagram are also confirmed by computing various correlators and chiral linear conductances of the system. In this way, our results find excellent agreement with many recent puzzling experimental results for the cases of $\nu_1=1/3$ and 1. We also discuss and make predictions for the case of a constriction system with $\nu_2=5/2$.

DOI: [10.1103/PhysRevB.77.035331](https://doi.org/10.1103/PhysRevB.77.035331)

PACS number(s): 73.23.-b, 71.10.Pm, 73.43.Jn

I. INTRODUCTION

Despite being a subject of intense experimental and theoretical interest, much is yet to be learned of the combined effects of electron correlations and impurities on the transport properties of low-dimensional strongly correlated systems. The availability of several nonperturbative theoretical methods for studying the physics of systems in one spatial dimension has, however, allowed for considerable progress to be made for such systems.¹ A physical one-dimensional system ideal for studying these issues are fractional quantum Hall edges (FQHEs).^{2,3} Considerable experimental advances have been made in exploring the physics of the edge states⁴ and in confirming many of the theoretical predictions made of the remarkable properties of these systems.⁵ Several recent experiments have, however, pointed out the need to develop a deeper theoretical understanding of interedge quasiparticle tunneling phenomena in FQHE systems with gate-voltage controlled constrictions.⁶⁻⁹ These experiments serve as the primary motivation for the models proposed in this work. However, before discussing these experiments, we first present a discussion of the existing theoretical paradigm for the understanding of interedge tunneling physics in FQHE systems.

Kane¹¹ and Fisher¹² observed in their classic work that (a) the tunneling between two fractional quantum Hall (FQH) edges separated by the FQH fluid was akin to the backscattering of electrons by an impurity in a Tomonaga-Luttinger liquid (TLL) and (b) the tunneling between two FQH bubbles separated by vacuum was akin to the tunneling of electrons across a weak link (infinitely high barrier) between two TLLs. Their perturbative analysis revealed that process (a) was relevant under renormalization group (RG) transformations, while process (b) was irrelevant, thus suggesting that the low-energy physics of the FQHE tunneling

problem was likely to be that of two FQH bubbles separated by vacuum. Both these scenarios are described by the boundary sine-Gordon model.¹³ In the following years, a quantum Monte Carlo simulation by Moon *et al.*,¹⁴ an instanton calculation by Furusaki and Nagaosa,¹⁵ a conformal field-theory analysis by Wong and Affleck,¹⁶ and the exact solution of Fendley *et al.*¹⁷ using the thermodynamic Bethe ansatz method demonstrated that these scenarios were, in fact, correct in their description of the system. Further, they showed that, within the confines of the boundary sine-Gordon model, there was no intermediate fixed point in the RG flow of the backscattering/tunneling couplings in this model. Several works have also analyzed the effects of interedge interactions¹⁸⁻²⁰ and disorder²¹ on quasiparticle transport in FQH edge systems. Attention has also been given to tunneling at point contacts between FQH fluids with different filling fractions²² as well as at contacts with Fermi liquid reservoirs.²³ More recently, attempts have been made at developing a more general theory for the study of critical points in edge tunneling between generic FQH states.^{24,25} Interestingly, the boundary sine-Gordon model has also been found to be relevant to the physics of Josephson junction SQUID systems.²⁶

The phenomenological description of tunneling between chiral edges outlined above relies on the following scenario. For no backscattering coupling between the two edges of opposite chirality at, say, $x \sim 0$, we have a system of two chiral one-dimensional (1D) systems which are continuous at $x=0$. This can be seen by consulting Fig. 1 for the case of the fields $(\phi_{1,in}, \phi_{1,out})$ and $(\phi_{2,in}, \phi_{2,out})$ being continuous. Upon introducing a small RG-relevant interedge tunnel coupling, we are left at strong backscattering coupling with a system in which the earlier edges are now discontinuous across $x=0$; they have, in fact, now become reconnected in a different configuration, with the fields $(\phi_{1,in}, \phi_{2,out})$ and $(\phi_{2,in}, \phi_{1,out})$

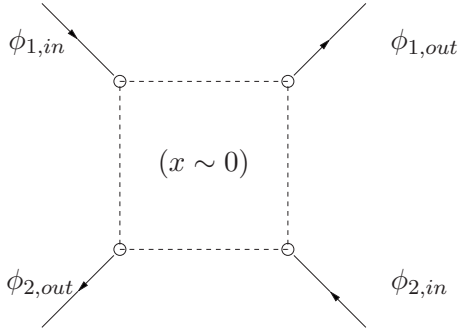


FIG. 1. A schematic diagram of the “boundary” in our system given by the dashed box around the region symbolized by $(x \sim 0)$. The four chiral fields approaching and leaving this region are shown by the arrows marked as $\phi_{1,in}$, $\phi_{1,out}$, $\phi_{2,in}$, and $\phi_{2,out}$. The dashed horizontal and vertical lines at the junction represent quasiparticle transmission in various directions.

now being continuous (as can be seen in Fig. 1). This means that in order to describe ballistic transport intermediate between these two which is characterized by a finite backscattering of current, one must consider the possibility of the fields describing the chiral edge excitations as being discontinuous across $x=0$. In doing so, it appears necessary to rely on ideas nonperturbative in nature. Accounting for additional quasiparticle tunneling among the various incoming and outgoing chiral edges is then likely to lead to a nontrivial variation of the boundary sine-Gordon model. Insights on these issues were gained recently in Ref. 27, in the form of a new model for the constriction geometry in a quantum Hall system which, while being simple in essence, is clearly beyond the paradigm of the quantum point contact. We aim here to develop the ideas presented in that work, exploring more fully the consequences of such a constriction system.

As will be discussed in the next section, several recent experiments on interedge tunneling in FQHE systems show that it is possible to use the voltage of a split-gate constriction to tune the interedge transmission to values intermediate to those in the two scenarios described above. Further, they reveal a very interesting evolution of the transmission through the constriction with decreasing interedge bias. This will lead us to formulate a simple phenomenological model for the split-gate constriction region. We will then perform a Landauer-Buttiker analysis and compute the conductances of the model. The results of this analysis will be seen to point to some interesting conclusions for transport in the presence of a constriction. It is now well established that the low-energy theory for the dynamics of the gapless long-wavelength excitations on the edges of a FQH system is described by a hydrodynamic continuum chiral TLL theory² of propagating density disturbances which are bosonic in nature. Adhering to the spirit of such a hydrodynamic description, we formulate a continuum model for the constricted quantum Hall edge system in Sec. III. In Sec. IV, we introduce local quasiparticle tunneling processes inside the constriction and construct a boundary theory for the problem. In this way, we investigate the RG phase diagram of the system for the various tunnel couplings. We complete the study in Sec. V by computing several chiral correlators and conductances at

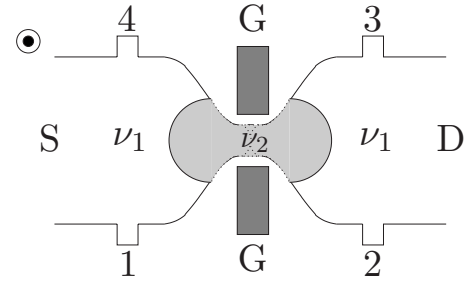


FIG. 2. A schematic diagram of a FQH bar with a gate-voltage (G) controlled split-gate constriction that lowers the electronic density in the constriction region as well as brings the top and bottom edges of the Hall fluid in close proximity, allowing for tunneling to take place between the opposite edges. S and D signify the source and drain ends of the Hall bar, while the numbers 1–4 signify the current/voltage lead connections. The external magnetic field points out of the plane of the paper.

weak- and strong-quasiparticle tunnel coupling values. We then present a comparison of the results of our model with those obtained from recent experiments in Sec. VI. Here, we will also reflect on the relevance of our model to the case of a constriction with a filling factor of $\nu=5/2$. We end by discussing some finer aspects of the model and outlining some open directions in Sec. VII.

II. MODEL FOR A SPLIT-GATE CONSTRICTION

We now propose a simple, phenomenological model for a split-gate constriction created in a quantum Hall system. A schematic diagram of an experimental setup of a FQH bar with a gate-voltage controlled constriction is shown in Fig. 2.

As is indicated in Fig. 2, the constriction is created electrostatically in a two-dimensional electron gas (2DEG) quantum Hall system at filling fraction ν_1 by the electronegative gating of metallic split gates. An important effect of the split-gate constriction is to bring the two counterpropagating edges of the Hall fluid in close proximity, allowing for the possibility for quasiparticles to tunnel between them. As discussed earlier, this has been a major focus in the study of the physics of FQHE systems. However, an often neglected effect of the split gates is that the electric field induced by them reduces the 2DEG density (and, hence, the filling fraction of the Hall fluid) in the narrow constriction region; the interparticle correlations in the constriction are, thus, likely to increase in strength. We can, therefore, expect the filling fraction of the FQH fluid in the constriction, ν_2 , to be a function of ν_1 as well as the gate voltage V_g , i.e., $\nu_2 \equiv \nu_2(\nu_1, V_g)$, in such a way that (i) $\nu_2 = \nu_1$ for $V_g = 0$ (i.e., no constriction) and (ii) $\nu_2 < \nu_1$ for $V_g < 0$ (i.e., with a constriction). While the filling factor ν_1 (for ν_1^{-1} being an odd integer, such that we have only single edge states) can be related to the strength of the interedge density-density interactions, g_{edge} , in the bulk of the FQH system^{3,12,22}

$$\nu_1 = (1 + g_{edge})^{-1/2}, \quad (1)$$

no such simple relation exists, at present, for the filling factor in the constriction, ν_2 . Clearly, this will need a greater un-

derstanding of the role of the gate voltage V_g in creating the constriction.

A. Surprises from the experiments

We now turn to a discussion of the several puzzling results observed in experiments on transport through split-gate constrictions in integer⁶ and fractional^{7,8} quantum Hall systems, and outline the several intriguing results observed therein. Working with an experimental setup as shown in Fig. 2, a finite dc bias between the two edges coming toward the constriction V_c is imposed through the source (S) terminal while the drain (D) terminal as well as terminals 1 and 2 are kept grounded.

(i) A current I is incident on the constriction from the upper-left edge and is partially transmitted, with the transmitted current finally being collected at terminal 3. The reflected current is collected at terminal 1 and gives rise to a bias-independent longitudinal differential resistance across the constriction at large bias V_c .

(ii) The two-terminal differential conductance $G(V_c)$ is measured at temperatures as low as $250 \text{ mK} < eV_c$, and gives the transmission coefficient of the constriction $0 \leq t(V_c) [= G(V_c)/G_0] \leq 1$, where $G_0 = \nu_1 e^2/h$ is the Hall conductance of the bulk, $\nu_1 = 1$ in Ref. 6, and $\nu = 1/3$ in Refs. 7 and 8]. At sufficiently large values of the gate voltage V_g and large bias V_c , $t(V_c)$ is observed to saturate with $|V_c|$ at a value less than unity. Further, $t(V_c)$ is observed to dip sharply and vanish with a power-law dependence on V_c as $|V_c| \rightarrow 0$. A comparison with the theory of interedge Laughlin quasiparticle tunneling developed by Fendley *et al.*¹⁷ suggests strongly that the constriction transmission is governed by the local filling factor of the Hall fluid in the constriction, even though this region is likely to be small in extent. This is unexpected for the case of the bulk being in an integer quantum Hall state⁶ where edge transport is understood in terms of noninteracting electron charge carriers.

(iii) A particularly intriguing observation is that of the evolution of the constriction transmission $t(V_c)$ at very low temperatures (e.g., 50 mK) as the split-gate voltage V_g is varied in the limit of vanishing interedge bias V_c . While $t(V_c)$ shows a zero-bias minimum at sufficiently large V_g , decreasing V_g leads to a bias-independent transmission at a particular value of V_g and then to an enhanced zero-bias transmission for yet lower values of V_g . The same behavior of the zero-bias transmission is also observed by holding the gate voltage V_g fixed and lowering the temperature from 700 to 50 mK. For the case of $\nu_1 = 1$, the bias-independent transmission is observed at a value of $t^* = 1/2$,⁶ while for $\nu_1 = 1/3$, it is observed at $t^* = 3/4$.^{7,8} A similar enhancement of the zero-bias transmission at sufficiently weak gate voltages was also reported for the case of bulk filling fractions $\nu_1 = 2/5$ and $3/7$.⁸ The bias independence as well as the enhancement of the transmission $t(V_c)$ are quite unexpected from the viewpoint of the theoretical framework of edge tunneling described earlier.

(iv) The constriction transmission for a bulk $\nu = 2$ system displayed two dip-to-peak evolutions, with bias-independent behaviors observed at $t^* = 1/4$, $1/2$, and $3/4$.⁶ This appears

to indicate the independent effects of the two edge modes in the $\nu = 2$ system.

(v) Varying considerably the size and shape of the metallic gates (which form the constriction region) did not appear to affect the dip-to-peak nature of the evolution of the constriction transmission with the strength of the gate voltage.¹⁰

Let us now consider the probable effects of a split-gate voltage constriction. Clearly, other than promoting the tunneling of quasiparticles between oppositely directed edges (due simply to enhanced wave function overlap due to the proximity of the edges), the more noteworthy effect is likely to be the creation of a smooth and long constriction potential, which depletes the local electronic density (and, hence, lowers the local filling factor) locally from its value in the bulk. Indeed, this led Roddaro *et al.*⁶ to conjecture on the possibility of a small region in the neighborhood of the constriction with a reduced filling factor ($\nu_2 < \nu_1$) as the cause of their puzzling results (see Fig. 2). This conjecture, however, remained unsubstantiated by the formal analysis of a concrete theoretical model. Thus, their explanations for the $\nu = 1$ system remained suggestive at best and no attempts at unifying the observations at both integer and fractional values of ν were made. Thus, the pressing questions that remain to be answered are as follows. What drives the gate-voltage tuned insulator-metal transition at vanishing edge bias in the constriction system (as evidenced by the dip-to-peak evolution with decreasing strength of the gate voltage)? Can purely local interedge quasiparticle tunneling processes, which need an interplay of impurity scattering and electronic correlations,¹¹ be the sole cause? Is there a symmetry governing the edge-bias-independent response of the constriction transmission at a critical value of the constriction filling factor (as seen by tuning the gate voltage)? If the system is indeed critical at this point, what does its gapless theory look like?

At the same time, earlier theoretical efforts^{28–30} were unable to provide any simple explanations of these experimental observations. Most notably, the scenario proposed in Ref. 28 involved the complications of stripe states arising from longer range interactions. However, it failed to present any mechanism in explaining the evolution of g with V_G . The same is also true of proposals of line junctions²⁹ as well as the effects of interedge interactions on quasiparticle tunneling.³⁰ Thus, keeping in mind that the theory of Refs. 11 and 17 matches the experiments in only a very restricted parameter regime, the lack of a clear theoretical understanding remained an important problem to be addressed. The creation of a model with an effort toward explaining the puzzles was, therefore, the main motivation of an earlier work.²⁷ In what follows, this model is first formulated and then analyzed in detail.

B. Landauer-Buttiker analysis of transport

Inspired by these experimental findings, we build, in the remainder of this section, a simple phenomenological model of a FQH split-gate constriction with a reduced local filling fraction. In this way, we aim to provide a qualitative understanding of some of the observations discussed above. Fur-

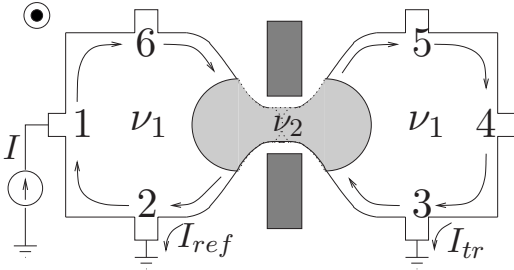


FIG. 3. A schematic diagram of a QH bar constriction circuit, with the filling factors of the bulk and constriction regions being ν_1 and ν_2 , respectively. The numbers 1–6 signify the various current and voltage terminals. The current I is sent into the circuit at terminal 1 by the current source, while the current transmitted through (I_{tr}) and the current backscattered from (I_{ref}) the constriction are received at terminals 3 and 2, respectively. The external magnetic field points out of the plane of the paper.

thermore, certain elements of this simple model will then be employed as input parameters in a more sophisticated theory involving bosonic edge excitations in subsequent sections, in providing explanations of some of the other, more puzzling, experimental results. The analysis of this model will be carried out in two ways. The first will involve an explicit calculation of the various Landauer-Buttiker conductances of the measurement geometry. In the second analysis, we will show how the results of the explicit calculation can be derived more simply by making two assumptions of the system at hand.

We begin by performing a Landauer-Buttiker analysis of the edge circuit.³¹ This is shown in Fig. 3. The central feature of our model is the region of lowered filling factor (ν_2) assumed to be created by the split-gate constriction gates. Let us now estimate the spatial extent, L_{con} , of the ν_2 region. This can be done by noting that the transport data taken at a temperature of 50 mK does not appear to show any interference effects arising from coherence across the entire constriction.⁶ Thus, L_{con} can be safely assumed to be longer than the thermal length $L_T = \hbar v / k_B T$ (where v is the edge velocity). For a typical $v = 10^3 \text{ ms}^{-1}$ (Ref. 32) and $T = 50 \text{ mK}$, $L_T \sim 1 \mu\text{m}$. Clearly, $L_{con} (> 1 \mu\text{m}) \gg$ magnetic length $l_B (\sim 100 \text{ \AA})$, justifying our assumption of the mesoscopic nature of the ν_2 region.

In a Landauer-Buttiker analysis,³³ the net currents flowing in the various arms are assumed to satisfy linear relations with the applied voltages (valid for small values of the voltages), with the proportionality factors being the various transmission coefficients for the quantum system. Solving the various linear relations between the currents and voltages gives us the various conductances of the system. It is helpful to use the fact that the net current for voltage probes is zero, and that we have the freedom to set the voltage of one of the terminals to zero (as currents are related to applied voltage differences). Thus, in Fig. 3, we set $V_4 = 0$, and since terminals 4, 5, and 6 are voltage probes, $I_4 = 0 = I_5 = I_6$. When put together with the fact that terminals 2 and 3 were grounded in the experiments,⁶ i.e., $V_2 = 0 = V_3$, this allows us to exclude the current-voltage relation for terminal 4 altogether (i.e., remove one row from the transmission matrix linking the

currents and voltages). Thus, we can write the current-voltage relations in matrix form as

$$\mathbf{I} = \bar{\mathbf{T}}\mathbf{V}, \quad (2)$$

where the current and voltage column vectors are $\mathbf{I} = (I_1, I_2, I_3, I_5, I_6)$ and $\mathbf{V} = (V_1, V_2, V_3, V_5, V_6)$, respectively, and the $\bar{\mathbf{T}}$ transmission matrix is given by

$$\bar{\mathbf{T}} = \begin{pmatrix} \nu_1 & -\nu_1 & 0 & 0 & 0 \\ 0 & \nu_1 & -\nu_2 & 0 & -\nu_{ref} \\ 0 & 0 & \nu_1 & -\nu_1 & 0 \\ 0 & 0 & -\nu_{ref} & \nu_1 & -\nu_2 \\ -\nu_1 & 0 & 0 & 0 & \nu_1 \end{pmatrix},$$

where ν_{ref} is the transmission coefficient for the current backscattered from the constriction. We now solve these linear relations. Measuring all voltages with respect to terminal 4 (which we have set to zero), we can see that as $I_6 = 0$, we find $V_6 = V_1$. Further, from $I_5 = 0$, we get

$$V_5 = \frac{\nu_2}{\nu_1} V_6 = \frac{\nu_2}{\nu_1} V_1. \quad (3)$$

The current leaving the circuit at terminal 3 is given by $I_3 = -I_{tr} = -\nu_1 V_5$ (where I_{tr} is the current transmitted through the constriction region from terminal 6 to terminal 5). This gives us

$$I_{tr} = \nu_1 \frac{\nu_2}{\nu_1} V_1 = \nu_2 V_1. \quad (4)$$

In a similar manner, we can compute the current leaving the circuit at terminal 2 (which, with terminal 3 being grounded, consists entirely of the current backscattered from the constriction) as $I_2 = -I_{ref} = -\nu_{ref} V_6$. Then, from overall current conservation in our circuit, the total injected current is given by $I_1 = \nu_1 V_1 = I_{tr} + I_{ref}$, which gives us

$$I_{ref} = (\nu_1 - \nu_2) V_1. \quad (5)$$

This leads us to $\nu_{ref} = \nu_1 - \nu_2$. This expression for ν_{ref} can also be found very simply by noting that the constraint of unitarity for the transmission matrix means that the sum of the elements in every row (or every column) must add up to zero.³³ We can now also compute the conductance (in units of e^2/h) due to the current backscattered from the constriction as

$$G^{back} = \frac{I_{ref}}{V_1} = \nu_1 - \nu_2. \quad (6)$$

This also gives us the ‘‘background’’ (BG) value of the resistance drop across the constriction as

$$R^{BG} = \frac{V_6 - V_5}{I_1 - I_5} = \frac{G^{back}}{\nu_1^2}. \quad (7)$$

Having carried out the Landauer-Buttiker analysis, we now show how all of the results obtained therein can be rederived through a simple analysis of the circuit which relies on essentially two assumptions on the nature of the sys-

tem at hand and the conservation of current.²⁷ This will allow us to reflect on the simplicity and efficiency of the assumptions. Thus, let us begin by stating the assumptions made and show how they lead in a straightforward way to simple relations for several physical quantities measured in the experiment. These are the following:

(i) The voltage bias between the two edges of the sample (i.e., the Hall voltage for the system being in a quantum Hall state) is not affected by the local application of a gate voltage at a constriction as long as the bulk of the system is in an incompressible quantum Hall state with filling fraction ν_1 .

(ii) The two-terminal conductance measured across the constriction is determined by the current transmitted through it, which in turn is governed by the filling fraction of the Hall fluid in the constriction, ν_2 . This needs the breakup of the current coming toward the constriction to take place at the boundary and constriction Hall fluid regions (which is sufficiently far away from the center of the constriction region).

Thus, by denoting the current injected into the system from the source terminal as I , we know that $I = G_b V_{63}$, where $G_b = \nu_1 e^2/h$ is the bulk Hall conductance and V_{63} is the edge bias. From assumption (ii), by denoting the current transmitted through the constriction as I_{tr} , it is clear that $I_{tr} = G_c V_{63}$, where $G_c = \nu_2 e^2/h$ is the two-terminal conductance measured across the constriction. Putting these two relations together using assumption (i), we obtain the transmitted current I_{tr} in terms of the incoming current I as

$$I_{tr} = \frac{G_c}{G_b} I = \frac{\nu_2}{\nu_1} I. \quad (8)$$

Thus, we see that our assumptions give us a very simple relation for the splitting ratio γ for the currents at the constriction (which is simply related to the transmission coefficient of the constriction discussed above for no interedge tunneling) as being $\gamma = \nu_2/\nu_1$. Now, from Kirchoff's law for current conservation, we get the current reflected at the constriction $I_{ref} = I - I_{tr} = (1 - \nu_2/\nu_1)I$. This then gives the minimum value of the backscattering conductance as

$$G^{back} = I_{ref}/V_{63} = (1 - \nu_2/\nu_1)G_b = (\nu_1 - \nu_2)(e^2/h). \quad (9)$$

G^{back} is simply related to the reflection coefficient of the constriction for no interedge tunneling, and shows that the *effective* filling fraction governing G^{back} is $\nu_{ref} = \nu_1 - \nu_2$. Now, with the current at terminal 5, I_5 , being the transmitted current I_{tr} , we get $I_5 = G_b V_5 = I_{tr} = G_c V_6$ (since $V_3 = 0$), giving $V_5 = (G_c/G_b)V_6$. We then find the background value of the longitudinal resistance drop across the constriction to be

$$R^{BG} = \frac{V_6 - V_5}{I_1 - I_5} = \left(1 - \frac{\nu_2}{\nu_1}\right) G_b^{-1}, \quad (10)$$

which arises from the partial reflection and transmission of the incoming edge current due to the mismatch of the filling fraction in the bulk and constriction regions. The experimentally obtained value for R^{BG} is, in fact, used by the authors of Refs. 6 and 7 to determine the value of the constriction filling factor ν_2 from Eq. (10). Further, we can see that G^{back} and R^{BG} are simply related by $G^{back} = G_b^2 R^{BG}$. More generally, the differential longitudinal drop across the constriction

dV_{65}/dI is related to (and also experimentally determined in Ref. 7) the differential backscattering conductance dI_{ref}/dV_{63} by the simple relation, as seen earlier,

$$\frac{dI_{ref}}{dV_{63}} = G_b^2 \frac{dV_{65}}{dI}. \quad (11)$$

Further, we also check that the Hall conductances measured on the two sides of the constriction are determined by ν_1 alone,

$$\frac{I_{tr}}{V_{53}} = G_b = \frac{I}{V_{62}}. \quad (12)$$

Thus, we see that by allowing for the constriction region to have a reduced filling fraction (ν_2) than that of the bulk (ν_1) and making the two assumptions stated above, we are able (i) to find a simple expression for the splitting ratio γ of the current incident on the constriction (or, the zeroth constriction transmission coefficient) as well as (ii) find an expression for the longitudinal resistance drop across the constriction which arises from the breakup of the current.

At the heart of these results lies the fact that a constriction region with a reduced filling fraction necessitates the transfer of charge from the incoming edge to the opposite outgoing edge via the incompressible bulk. Put another way, it becomes imperative to consider the nonconservation of edge current in studying transport across such a constriction. This is characterized by the presence of a current reflected at the boundary of the bulk and constriction regions in the model setup above. While charge dissipation away from the edge can be modeled in terms of quasiparticle tunneling at multiple point-contact junctions,^{23,34} such a mechanism appears to be incompatible with the experimental finding of an edge-bias-independent current reflected from the constriction region. The existence of a narrow gapless region of Hall fluid lying in between the incompressible bulk and constriction Hall fluid regions may well provide an answer: such a gapless region would act as a channel for the current reflected from the constriction region. It is, therefore, tempting to speculate on the possibility of a nonperturbative physical mechanism³⁵ of a chiral Tomonaga-Luttinger liquid undergoing charge dissipation along a short stretch of its length while in contact with a bath (the gapless region) as being the microscopic origin for the phenomenological model described above.

While there are ways of studying the electrostatic effects of a gate-voltage controlled constriction on the incompressible quantum Hall fluid,^{22,28} we have instead chosen a particularly simple and tractable path for modeling the edge structure which involves very few details pertaining to the bulk. The electrostatic calculations of Ref. 28 explore the possibility of edge reconstruction within the constriction region, i.e., long-range interactions between electrons in the quantum Hall ground state giving rise to a set of compressible and incompressible stripes at the edge.³⁶ In this work, however, we consider only short-ranged electron correlations, which cause the formation of the chiral TLL state without any intervening stripe states.² Further, we neglect the possibility of the formation of line-junction nonchiral TLLs

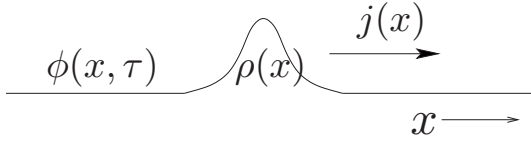


FIG. 4. A schematic diagram for the infinitely long right-moving quantum Hall edge state. The edge displacement is given by the bosonic field $\phi(x, \tau)$, while the edge density and current are given by $\rho(x, \tau) \sim \partial_x \phi$ and $j(x, \tau) \sim \partial_\tau \phi$, respectively.

across the vacuum regions in the shadow areas of the metallic gates,²⁹ focusing instead on the transmitted and reflected edge states arising from the nature of the Hall fluid inside the constriction. Thus, we devote our attention to short-ranged electronic correlations which cause the formation of chiral TLL edge states (without the intervention of any stripe states²⁸ arising from longer range interactions).

As we will see in the following sections, such a model of a constriction in a quantum Hall sample allows for considerable progress to be made in developing a (quadratic) effective field theory for the ballistic transport of current in terms of propagating chiral edge density-wave excitations. Interesting consequences for quasiparticle tunneling will then be shown to result from the exponentiation of these quadratic fields, in particular, giving rise to the competition between two RG-relevant quasiparticle tunneling operators which determine the fate of the low-bias transmission and reflection conductances through the constriction. In this way, we will show how our model is able to provide a qualitative understanding of the puzzling findings of the experiments mentioned above in a unified manner. While it appears difficult at first to formulate a continuum model describing a scenario of intermediate ballistic transmission of current through such a constriction by a quadratic bosonic field theory similar to that of Wen,² we find that considerable progress can be made by understanding the role of matching (or boundary) conditions in such a theory. In this way, we are able to set up in the following section a very general Hamiltonian, as well as action, formalism describing transport through such a constriction system.

III. CONTINUUM THEORY FOR THE CONSTRICTION SYSTEM

In this section, we develop a continuum theory for the model of the constriction system presented above. However, for the sake of clarity and continuity, we begin by presenting the basic ingredients of Wen's continuum theory for the infinitely long chiral Tomonaga-Luttinger liquid.²

A. Continuum theory for infinite chiral Tomonaga-Luttinger liquid

Wen's hydrodynamic formulation describes the excitations of such a system in terms of chiral bosonic density wave modes. The Hamiltonian (and the action) is quadratic in the bosonic field $\phi(x, \tau)$ (where τ is the Euclidean time) and has two parameters: the edge velocity v and the filling fraction ν . This is shown in Fig. 4.

The energy cost for density distortions of the edge of the quantum Hall system was shown by Wen to lead to a Hamiltonian (for, say, the right-moving edge of a Hall bar)

$$H = \frac{v}{4\pi\nu} \int_{-\infty}^{\infty} dx [\partial_x \phi_R(x, \tau)]^2. \quad (13)$$

The equal-time (Kac-Moody) commutation relation for the bosonic field ϕ_R is given by

$$[\phi_R(x), \partial_x \phi_R(x')] = i\pi\nu \delta(x - x'), \quad (14)$$

which makes $\partial_x \phi_R$ the momentum canonically conjugate to ϕ_R . The edge density distortion is given by $\rho(x) = \partial_x \phi_R(x) / 2\pi$ and the Hamilton equation of motion gives

$$i\partial_\tau \rho_R = i[H, \rho_R] = -v \partial_x \rho_R(x, \tau). \quad (15)$$

This gives us the density $\rho_R(x, \tau) = \rho_R(x + iv\tau)$. Further, from the equation of continuity

$$i\partial_\tau \rho + \partial_x j = 0, \quad (16)$$

we find the current density as $j_R = -i\partial_\tau \phi_R / 2\pi$. Fourier transforming the equation of motion gives us the expected linear dispersion relation for the edge density waves as $\omega = vk$. From the commutation relations, we obtain the Legendre transformation for the Hamiltonian $H(\phi_R)$. This leads to the Euclidean action for the chiral (right moving) TLL as

$$S_R = \frac{1}{4\pi\nu} \int_0^\beta d\tau \int_{-\infty}^{\infty} dx \partial_x \phi_R (i\partial_\tau + v\partial_x) \phi_R(x, \tau). \quad (17)$$

The Hamiltonian for the left-moving edge density wave is the same as that given above for $\phi_R \rightarrow \phi_L$, but the density $\rho_L = -\partial_x \phi_L / 2\pi$. As the equal-time commutation relation $[\phi_L(x), \partial_x \phi_L(x')] = -i\pi\nu \delta(x - x')$, the action for the left-moving edge chiral TLL has a Legendre transformation term $-i\partial_\tau \phi_L \partial_x \phi_L$.

B. Continuum theory for the constriction edge model

We now formulate a continuum theory for the constriction edge model discussed in Sec. II along the lines of Wen's hydrodynamic description given above. The aim will, therefore, be to develop a quadratic theory in bosonic fields in an edge model consisting of chiral, current carrying, gapless edge density-wave excitations describing ballistic transport through the transmitting and reflecting edge states surrounding the constriction region. This is shown in Fig. 5. As discussed earlier, such a model is critically needed in order to describe the experimentally observed scenario of intermediate ballistic transmission through the constriction.⁶ We take the spatial extent of the constriction region $2a$ to lie in the range $l_B \ll 2a \ll L$, where L is the total system size and l_B is the magnetic length; the external arms (in, \dots, out) meet the internal ones (u, \dots, l) at the four corners of the constriction. From our earlier discussions, it is also evident that ν_1 governs the properties of the four outer arms, while ν_2 that of the upper and lower (transmitted) arms of the circuit at the constriction. The effective filling factor for the right and left (reflected) arms of the circuit (ν_{ref}) is treated as a parameter

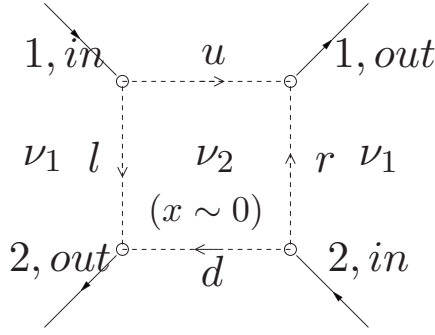


FIG. 5. A schematic diagram of the “constriction” system given by the dashed box around the region $x \sim 0$ and symbolized by the filling fraction ν_2 lower than that of the bulk, ν_1 . The four chiral fields approaching and leaving this region are shown by the arrows marked as 1, *in*, 1, *out*, 2, *in*, and 2, *out*. The dashed horizontal and vertical lines at the junction represent the edge states which are transmitted (u, d) and reflected (l, r) at the constriction, respectively.

to be determined. We focus in this work on the effects of a changing filling fraction, keeping the edge velocity v the same everywhere.

We will now set forth the Hamiltonian formulation of the model. This approach will elucidate the importance of matching (or boundary) conditions in providing a correct and consistent description of the dynamics of the system.²⁷ We will follow this up by providing the more elegant formulation of the problem based on the action, showing how the information content of the boundary terms is already included in this language.

1. Hamiltonian formulation and matching conditions

The energy cost for chiral density-wave excitations that describe ballistic transport in the various arms of the circuit shown in Fig. 5 is given by a Hamiltonian $H = H^{ext} + H^{int}$, where

$$H^{ext} = \frac{\pi v}{\nu_1} \left[\int_{-L}^{-a} dx (\rho_{1in}^2 + \rho_{2out}^2) + \int_a^L dx (\rho_{2in}^2 + \rho_{1out}^2) \right],$$

$$H^{int} = \frac{\pi v}{\nu_2} \int_{-a}^a dx (\rho_u^2 + \rho_d^2) + \frac{\pi v}{\nu_{ref}} \int_{-a}^a dy (\rho_r^2 + \rho_l^2). \quad (18)$$

The densities ρ are, as usual, represented in terms of bosonic fields ϕ describing the edge displacement,²

$$\begin{aligned} \rho_{1in} &= 1/2 \pi \partial_x \phi^{1in}, & \rho_{1out} &= 1/2 \pi \partial_x \phi^{1out}, \\ \rho_{2in} &= -1/2 \pi \partial_x \phi^{2in}, & \rho_{2out} &= -1/2 \pi \partial_x \phi^{2out}, \\ \rho_u &= 1/2 \pi \partial_x \phi^u, & \rho_d &= -1/2 \pi \partial_x \phi^d, \\ \rho_l &= 1/2 \pi \partial_y \phi^l, & \rho_r &= -1/2 \pi \partial_y \phi^r. \end{aligned} \quad (19)$$

The commutation relations satisfied by these fields are familiar

$$\begin{aligned} [\phi^{1in}(x), \partial_x \phi^{1in}(x')] &= i\pi \nu_1 \delta(x - x') \\ &= -[\phi^{2out}(x), \partial_x \phi^{2out}(x')], \end{aligned}$$

$$\begin{aligned} [\phi^{1out}(x), \partial_x \phi^{1out}(x')] &= i\pi \nu_1 \delta(x - x') \\ &= -[\phi^{2in}(x), \partial_x \phi^{2in}(x')], \end{aligned}$$

$$[\phi^u(x), \partial_x \phi^u(x')] = i\pi \nu_2 \delta(x - x') = -[\phi^d(x), \partial_x \phi^d(x')],$$

$$[\phi^l(y), \partial_y \phi^l(y')] = i\pi \nu_{ref} \delta(y - y') = -[\phi^r(y), \partial_y \phi^r(y')]. \quad (20)$$

Further, the Hamiltonian equations of motion derived from H again describe the ballistic transport of chiral edge density waves,

$$(\partial_t - v \partial_x) \rho^{1in}(x, t) = 0 = (\partial_t - v \partial_x) \rho^{1out}(x, t),$$

$$(\partial_t + v \partial_x) \rho^{2in}(x, t) = 0 = (\partial_t + v \partial_x) \rho^{2out}(x, t),$$

$$(\partial_t - v \partial_x) \rho^u(x, t) = 0 = (\partial_t + v \partial_x) \rho^d(x, t),$$

$$(\partial_t - v \partial_y) \rho^l(y, t) = 0 = (\partial_t + v \partial_y) \rho^r(y, t). \quad (21)$$

The H given above, however, needs to be supplemented with matching conditions at the corners of the constriction for a complete description. From the form of H , it is clear that we need two matching conditions at each corner; a reasonable choice is one defined on the fields and one on their spatial derivatives. We choose, for instance, at the top-left corner

$$\phi^{1in}(x = -a) = \phi^u(x = -a) + \phi^l(y = -a),$$

$$\partial_x \phi^{1in}(x = -a) = \partial_x \phi^u(x = -a) + \partial_y \phi^l(y = -a), \quad (22)$$

where x and y are the spatial coordinates describing the (1*in*, u) and l arms, respectively. Similarly, we choose the following matching conditions at the other three corners as

$$\phi^{1out}(x = a) = \phi^u(x = a) + \phi^r(y = -a),$$

$$\partial_x \phi^{1out}(x = a) = \partial_x \phi^u(x = a) + \partial_y \phi^r(y = -a),$$

$$\phi^{2in}(x = a) = \phi^d(x = a) + \phi^r(y = a),$$

$$\partial_x \phi^{2in}(x = a) = \partial_x \phi^d(x = a) + \partial_y \phi^r(y = a),$$

$$\phi^{2out}(x = -a) = \phi^d(x = -a) + \phi^l(y = a),$$

$$\partial_x \phi^{2out}(x = -a) = \partial_x \phi^d(x = -a) + \partial_y \phi^l(y = a). \quad (23)$$

The equation of continuity leads to the familiar form for the current operator $j^\alpha = -i \partial_r \phi^\alpha / (2\pi)$, where $\alpha = (1in, 1out, \dots, l, r)$. Thus, we can easily see that current conservation at every corner arises from the matching conditions on the bosonic fields ϕ . While the transmitting chiral edge modes convey a finite current across the constriction, the reflecting chiral edge modes convey a finite “backscattered” current across the sample. In this way, we formally establish the intermediate ballistic transmission scenario as

observed in the experiments. Charge density fluctuations at each corner are described by the matching conditions on $\partial_x \phi$. This matching condition is a statement of the conservation of net charge density at each corner. In this way, the two sets of matching conditions together establish the continuity of current and charge density at every corner of the junction system.

Using Eqs. (22), we compute the commutation relation

$$[\phi^l, \partial_y \phi^l]_{y \rightarrow -a} = ([\phi^{1in}, \partial_x \phi^{1in}] - [\phi^u, \partial_x \phi^u])_{x \rightarrow -a}, \quad (24)$$

giving us $\nu_{ref} = \nu_1 - \nu_2$. The commutation relation for $\phi^r(y \rightarrow a)$ similarly yields $\nu_{ref} = \nu_1 - \nu_2$ once again. This is in conformity with our result for ν_{ref} from the Landauer-Buttiker calculation. We now demonstrate explicitly that the cases of a perfect Hall bar ($\nu_2 = \nu_1$) and two Hall bubbles separated by vacuum ($\nu_2 = 0$) can be modeled as special limiting cases of the matching conditions [Eqs. (22)] given earlier. For $\nu_1 = \nu_2$, the commutation relation of the reflecting edge states vanishes, killing its dynamics. This can also be understood within a hydrodynamic prescription,² where a vanishing effective filling factor [the amplitude of the Kac-Moody commutation relation, Eq. (20)] leads to a diverging energy cost for edge charge density fluctuations; the dynamics of the bosonic field characterizing such fluctuations is, thus, completely damped. Thus, the reflecting edge states carry no current, while the transmitting edge states perfectly transmit all incoming current into the outgoing arms on the *opposite* side of the constriction. The matching conditions [Eqs. (22)] at the four corners are then reduced to

$$\begin{aligned} \phi^{1in}(x = -a) &= \phi^u(x = -a), & \phi^u(a) &= \phi^{1out}(x = a), \\ \phi^{2in}(x = a) &= \phi^d(x = a), & \phi^d(-a) &= \phi^{2out}(x = -a), \\ \partial_x \phi^{1in}(-a) &= \partial_x \phi^u(-a), & \partial_x \phi^u(a) &= \partial_x \phi^{1out}(a), \\ \partial_x \phi^{2in}(a) &= \partial_x \phi^d(a), & \partial_x \phi^d(-a) &= \partial_x \phi^{2out}(-a). \end{aligned} \quad (25)$$

These identifications of the fields and their spatial derivatives lead to the continuity conditions which underpin the hydrodynamic theory of Wen^{2,11} for the case of the two infinite chiral edges (say, upper and lower) of a Hall bar (with filling factor ν_1), and Eq. (20) then reproduces the well-known Kac-Moody commutation relation everywhere along the edges. This is shown in Fig. 6.

Similarly, for the case of $\nu_2 = 0$, the commutation relation for the transmitting edge states vanishes, killing its dynamics: they carry no current, while the reflecting edge states perfectly convey all incoming current into the outgoing arms on the *same* side of the constriction. Thus, the matching conditions [Eqs. (22)] at the four corners are reduced to

$$\begin{aligned} \phi^{1in}(x = -a) &= \phi^l(y = -a), & \phi^l(a) &= \phi^{2out}(x = -a), \\ \phi^{2in}(x = a) &= \phi^r(y = a), & \phi^r(-a) &= \phi^{1out}(x = a), \\ \partial_x \phi^{1in}(-a) &= \partial_y \phi^l(-a), & \partial_y \phi^l(a) &= \partial_x \phi^{2out}(-a), \\ \partial_x \phi^{2in}(a) &= \partial_y \phi^r(a), & \partial_y \phi^r(-a) &= \partial_x \phi^{1out}(a). \end{aligned} \quad (26)$$

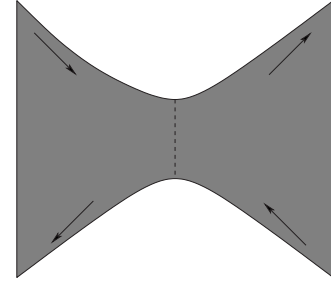


FIG. 6. A schematic diagram of the quantum Hall bar system with a constriction which promotes quasiparticle tunneling between two points on oppositely directed edges of the system (dashed line). The upper and lower edges are continuous everywhere and, therefore, have boundary conditions on the field ϕ and its spatial derivative $\partial_x \phi$ as given in Eqs. (25).

Again, these identifications of the fields and their spatial derivatives lead to the continuity conditions which underpin the hydrodynamic theory of Wen^{2,11} for the case of the infinite chiral edges (say, left and right) of two distinct Hall bubbles (each with filling factor ν_1) separated by vacuum, and again reproduce the familiar Kac-Moody commutation relations everywhere along the edges. This is shown in Fig. 7. We have, in this way, constructed a family of free theories describing ballistic transport through the constriction at intermediate transmission, with those of complete transmission and reflection representing two special cases. This represents an important advance in generalizing the quantum impurity model of Refs. 11 and 17.

2. Action formulation

In this section, we discuss the action (or Lagrangian) formulation of our problem. We will, in this way, demonstrate how the information content of the matching conditions above is already encoded in the action of the system in the forms of terms involving the local fields which are connected to one another by the matching conditions in the Hamiltonian formalism. Thus, we begin by writing down the action for the constriction model

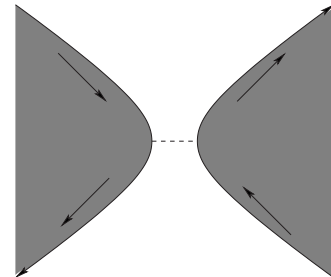


FIG. 7. A schematic diagram of a system of two quantum Hall droplets separated by vacuum and with a constriction which promotes electron tunneling between two points on adjacent (and oppositely directed) edges of the system (dashed line). The right and left edges are continuous everywhere and, therefore, have boundary conditions on the field ϕ and its spatial derivative $\partial_x \phi$ as given in Eqs. (26).

$$S = S_0 + S_1 + S_2, \quad (27)$$

where the action for the outer incoming and outgoing arms is

$$S_0 = \int_0^\beta d\tau \int_{-\infty}^{-a} dx \{ \mathcal{L}_0[\phi_i^{1,in}] + \mathcal{L}_1[\phi_i^{2,out}] \} \\ + \int_0^\beta d\tau \int_a^\infty dx \{ \mathcal{L}_0[\phi_i^{1,out}] + \mathcal{L}_1[\phi_i^{2,in}] \}, \quad (28)$$

where

$$\mathcal{L}_0[\phi^\alpha] = \frac{1}{4\pi} \partial_x \phi^\alpha (i\partial_\tau + v\partial_x) \phi^\alpha(x, \tau), \\ \mathcal{L}_1[\phi^\alpha] = \frac{1}{4\pi} \partial_x \phi^\alpha (-i\partial_\tau + v\partial_x) \phi^\alpha(x, \tau), \quad (29)$$

and we have normalized the entire action with regard to the bulk filling fraction ν_1 . Further, the action for the inner edges is

$$S_1 = \int_0^\beta \int_{-a}^a \left[\frac{f}{4\pi} \partial_x \phi^u (i\partial_\tau + v\partial_x) \phi^u(x, \tau) \right. \\ + \frac{f}{4\pi} \partial_x \phi^d (-i\partial_\tau + v\partial_x) \phi^d(x, \tau) \\ + \frac{g}{4\pi} \partial_y \phi^l (i\partial_\tau + v\partial_y) \phi^l(y, \tau) \\ \left. + \frac{g}{4\pi} \partial_y \phi^r (-i\partial_\tau + v\partial_y) \phi^r(y, \tau) \right], \quad (30)$$

where, by assuming that the properties of the upper and lower edge transmitted edge states of the constriction are determined by the effective filling fraction inside the constriction ν_2 , the quantity f is simply given by $f = \nu_1 / \nu_2$. The quantity $g = \nu_1 / \nu_{ref}$ (where ν_{ref} is the effective filling fraction for the reflected edge states on the left and right) will be determined from the analysis presently. It is worth noting that the same information can be obtained from the Hamiltonians [Eqs. (18)] and commutation relations [Eqs. (20)] together. Finally, the action for the corner nodes is given by

$$S_2 = - \int_0^\beta d\tau \int_{-a}^a dx \int_{-a}^a dy [\delta(x+a) \delta(y+a) \partial_x \phi^{1in} \{ (v\partial_x \phi^u \\ + \partial_y \phi^l) + i\partial_\tau (\phi^u + \phi^l) \} + \delta(x-a) \delta(y+a) \partial_x \phi^{1out} \{ (v\partial_x \phi^u \\ + \partial_y \phi^r) + i\partial_\tau (\phi^u + \phi^r) \} + \delta(x-a) \delta(y-a) \partial_x \phi^{2in} \{ (v\partial_x \phi^d \\ + \partial_y \phi^l) - i\partial_\tau (\phi^d + \phi^l) \} + \delta(x+a) \delta(y-a) \partial_x \phi^{2out} \{ (v\partial_x \phi^d \\ + \partial_y \phi^r) - i\partial_\tau (\phi^d + \phi^r) \}]. \quad (31)$$

We can now see the effects of these local terms in the action by computing the equations of motion for the various fields from the action. For the sake of brevity, we carry out this exercise at only the upper-left corner. The results obtained from the other three corners are precisely the same. Thus, we first compute the equation of motion of the ‘‘outer’’ field $\phi_{1in}(x=-a)$ by extremizing the action S with regard to $\partial_x \phi^{1in}(x=-a)$,

$$\frac{\delta S}{\delta(\partial_x \phi_{-a}^{1in})} = v(\partial_x \phi^{1in} - \partial_x \phi^u - \partial_y \phi^l) + i\partial_\tau (\phi^{1in} - \phi^u - \phi^l) = 0, \quad (32)$$

where we have suppressed the dependences of the fields on the spatial coordinates for the sake of compactness. From this, we can immediately see the matching conditions on ϕ and $\partial_x \phi$ at $(x=-a, y=-a)$ given earlier. We now compute the other two equations of motion at the top-left corner in the same way. We find, thus,

$$\frac{\delta S}{\delta(\partial_x \phi_{-a}^u)} = v(f\partial_x \phi^u - \partial_x \phi^{1in}) + i\partial_\tau (f\phi^u - \phi^{1in}) = 0, \\ \frac{\delta S}{\delta(\partial_y \phi_{-a}^l)} = v(g\partial_y \phi^l - \partial_x \phi^{1in}) + i\partial_\tau (g\phi^l - \phi^{1in}) = 0, \quad (33)$$

from which we can see that the currents $j^u(x=-a)$ and $j^l(y=-a)$ are given by

$$j^u(x=-a) = -i\partial_\tau \left(\phi^u + \frac{\phi^{1in}}{f} \right) = v \left(\phi^u - \frac{\phi^{1in}}{f} \right) \\ \equiv v\rho^u(x=-a), \\ j^l(y=-a) = i\partial_\tau \left(\phi^l + \frac{\phi^{1in}}{g} \right) = v \left(\phi^l - \frac{\phi^{1in}}{g} \right) \equiv v\rho^l(y=-a). \quad (34)$$

In the above relations, the currents (j^u, j^l) and corresponding densities (ρ^u, ρ^l) are those propagated from the incoming arm *1in* into the u(pper) and l(eft) edge states, respectively. Now, by applying Kirchoff’s law for the conservation of current (or, more generally, the equation of continuity) at the upper-left corner junction, $j^{1in}(x=-a) = j^u(x=-a) + j^l(y=-a)$, we obtain

$$\frac{1}{f} + \frac{1}{g} = 1, \quad (35)$$

which for $f = \nu_1 / \nu_2$ gives $g = \nu_1 / (\nu_1 - \nu_2)$. This, then, gives us the effective filling fraction of the reflected edge states as $\nu_{ref} = \nu_1 - \nu_2$. In this way, we can see that the action S contains all the information content given by the Hamiltonians together with the matching conditions.

IV. BOUNDARY THEORY FOR THE CONSTRICTION SYSTEM

In this section, we evaluate the role played by local inter-edge quasiparticle tunneling processes deep inside the constriction region in determining the fate of transport through the constriction. In order to do so, we proceed by first integrating out all bosonic degrees of freedom except the few involved in the tunneling processes. In this way, we are left with an effective *boundary* theory.¹¹ Given that we have a Gaussian action in terms of the bosonic fields, integrating out various bosonic degrees of freedom can be easily accom-

plished by performing Gaussian integrations^{1,13} (another analogous method involves using the solutions to the equations of motion^{11,37}). As this is a very standard procedure, we refer the reader to Refs. 1 and 13 for details. We pass instead to presenting the various boundary theories obtained in our model, revealing in turn the two interedge quasiparticle tunneling processes which compete in determining the low-energy dynamics of the system.

Now, as long as there is no quantum coherence across the constriction region, it is easily seen that the problem of weak, local quasiparticle tunneling between the upper (u) and lower (d) edges deep inside the constriction region (at, say, $x=0$) is exactly the same as that of local quasiparticle tunneling between the oppositely directed edges of a homogeneous quantum Hall bar with filling fraction ν_2 .¹¹ Importantly, the charge and statistics of the quasiparticles undergoing such tunneling processes should be governed by the local filling fraction ν_2 alone. Thus, in the action formalism presented earlier, such a quasiparticle tunneling process can be added to the action S by the term $\lambda_1 \cos(\sqrt{\nu_1}[\phi^u(0) - \phi^d(0)]) \equiv \lambda_1 \cos[\phi^{ud}(0)]$, where the tunnel coupling strength is given by λ_1 . Integrating out all bosonic degrees of freedom but $\phi^{ud}(x=0)$, we obtain the familiar Kane-Fisher type boundary theory¹¹

$$S_{ud} = \sum_{\bar{\omega}_n} \frac{|\bar{\omega}_n|}{2\pi\nu_2} |\phi_{\bar{\omega}_n}^{ud}(x=0)|^2 + \int d\tau \lambda_1 \cos[\phi^{ud}(x=0, \tau)]. \quad (36)$$

Applying a standard RG procedure, we find the RG equation for λ_1 as

$$\frac{d\lambda_1}{dl} = (1 - \nu_2)\lambda_1. \quad (37)$$

As $\nu_2 < 1$, the coupling λ_1 is found to be RG relevant and will grow under the flow to low energies and/or long length scales. Further, this quasiparticle tunneling process will clearly lower the transmission conductance across the constriction $g_{in,out}$ (for a source-drain bias as shown in Fig. 2).

We have, however, at least one other local quasiparticle tunneling process to account for: it is that between the left (l) and right (r) edges of the constriction and is revealed by the generalized quasiparticle-quasihole symmetry of the ground state in the lowest Landau level.^{27,38} This symmetry dictates that all properties of a quantum Hall system composed of quasiparticles in a partially filled lowest Landau level and with a filling factor ν_{qp} can be equivalently described by those of a quantum Hall system composed of quasiholes and with a filling factor $\nu_{qh} = 1 - \nu_{qp}$. This simple relation between ν_{qp} and ν_{qh} can be derived easily for the case of the filling factor (and, hence, electronic density) of the quantum Hall system deviating from a filling factor of $\nu_0 = 1/q$ (where $q = 2n+1 \in \mathcal{Z}$).³⁶ To see this, first, note that by increasing the electronic density of the system, we add q quasiparticles for each electron added. Then, for n_0 being the original electronic density, n_e the new increased electronic density, and n_{qp} the density of quasiparticles,

$$n_e = n_0 + \frac{n_{qp}}{q} = \frac{\nu_0}{2\pi l_B^2} + \frac{\nu_0 \nu_{qp}}{2\pi l_B^2}, \quad (38)$$

where l_B is the magnetic length and we have used $n_0 = \nu_0/2\pi l_B^2$. This gives us the quasiparticle filling factor ν_{qp} as

$$\nu_{qp} = \frac{\nu_e}{\nu_0}, \quad (39)$$

where $\nu_e = 2\pi l_B^2 n_e$ is the electronic filling factor. A similar calculation for the case of an equally lowered value of the electronic density n_e can also be carried out. We must now remember that we add q quasiholes to the system for every electron removed. Then, by following the same line of arguments, we get the quasihole filling factor ν_{qh} as

$$\nu_{qh} = 1 - \frac{\nu_e}{\nu_0} = 1 - \nu_{qp}. \quad (40)$$

Thus, we can see that ν_{qp} and ν_{qh} are related by a quasiparticle-quasihole conjugation transformation. Further, for the case of $\nu_0 = 1$, $\nu_{qp} = \nu_e$ and $\nu_{qh} = \nu_h = 1 - \nu_e$ are the well-known electron and hole conjugation symmetric filling factors with respect to the completely filled lowest electronic Landau level.³⁸

The application of this symmetry to the constriction model with a spatially dependent filling fraction relies on (a) the fact that the fractional (integer) quantum Hall ground state in the bulk of the system can be thought of as the completely filled effective lowest Landau level of quasiparticles (electrons), (b) that this state is protected by an energy gap which is larger than all other energy scales in the problem, and (c) there is no Landau level mixing. While the argument for a constriction circuit with the bulk being in the integer quantum Hall state of $\nu_1 = 1$ has been given in Ref. 6, a generalization for any constriction circuit with a general bulk filling factor $\nu_1 < 1$ was presented in Ref. 27. The argument is recounted below and encapsulated in Fig. 8.

By scaling the filling factors of all regions by ν_1 , we now have the effective filling factor of the bulk as 1, and that of the quantum Hall ground state inside the constriction region as the relative filling fraction $f^{-1} = \nu_2/\nu_1$. Carrying out the quasiparticle-quasihole conjugation transformation, we go to a system of holes (with the direction of the external magnetic field unaffected), but with the relative filling fraction of the constriction now given by $g^{-1} = 1 - f^{-1}$. We can then map this system of quasiholes onto that of time-reversed quasiparticles (i.e., quasiparticles in an oppositely directed external electromagnetic field). Finally, by rotating the system by 180° around the axis of the two outgoing current directions, we are left with a system of electrons with the external magnetic field pointing in the original direction. This final system is, however, crucially different in two ways from the original one. First, the filling factor of the fractional quantum Hall ground state inside the constriction region has, as noted earlier, changed from f^{-1} to $g^{-1} = 1 - f^{-1}$. Second, the directions of transmitted and reflected currents have been interchanged in going from the original system to the final one. It is easy to show that current conservation dictates that⁶

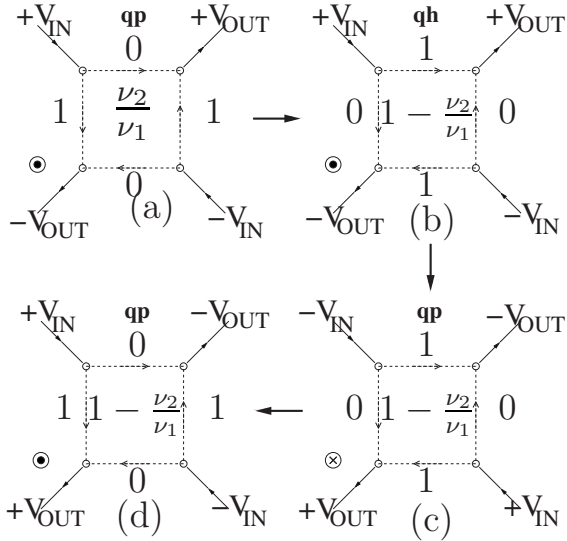


FIG. 8. The quasiparticle-quasihole (qp-qh) symmetry of the (ν_1, ν_2) constriction geometry in terms of the relative filling factor. The source-drain bias $2V_{in}$ is applied to the two incoming arms, while $\pm V_{out}$ are the equilibration potentials of the two outgoing arms. See text for a detailed description of the transformations linking (a) to (d).

$$I_{f-1} + I_{g-1} = 2\nu_1 \frac{e^2}{h} V_{in}, \quad (41)$$

where I_{f-1} and I_{g-1} are the transmitted currents in the original system and the final system after the mappings (i.e., the reflected current in the original system). Relations can also be written down in terms of differential transmission $t = dI/dV$ and reflection r (in units of $\nu_1 e^2/h$)

$$\begin{aligned} t_{f-1} &= 1 - t_{g-1} = r_{g-1}, \\ t_{g-1} &= 1 - t_{f-1} = r_{f-1}. \end{aligned} \quad (42)$$

This argument also clearly demonstrates that the local tunneling process that transports these quasiholes between the left (l) and right (r) edges of the constriction system is governed by the effective filling fraction of $g^{-1} = 1 - \nu_2/\nu_1$. Thus, we denote such a local tunneling process (again, chosen at $y=0$) on the l and r edges by a weak tunnel coupling λ_2 and a term in the action S , $\lambda_2 \cos[\phi^l(0) - \phi^r(0)] \equiv \lambda_2 \cos[\phi^{lr}(0)]$. Integrating out all bosonic degrees of freedom but $\phi^{lr}(y=0)$, we obtain another Kane-Fisher type boundary theory¹¹

$$S_{lr} = \sum_{\bar{\omega}_n} \frac{|\bar{\omega}_n|}{2\pi g} |\phi_{\bar{\omega}_n}^{lr}(y=0)|^2 + \int d\tau \lambda_2 \cos[\phi^{lr}(y=0, \tau)]. \quad (43)$$

Thus, we can see that the RG equation for the coupling λ_2 is given by

$$\frac{d\lambda_2}{dl} = \left(1 - \frac{1}{g}\right) \lambda_2 = \left[1 - \left(1 - \frac{\nu_2}{\nu_1}\right)\right] \lambda_2 = \frac{\nu_2}{\nu_1} \lambda_2. \quad (44)$$

As both $(\nu_1, \nu_2) > 1$ and $\nu_2 < \nu_1$, we can see that the coupling λ_2 is also RG relevant and will grow under the flow to low

energies and/or long length scales. Further, this tunneling process will increase the transmission conductance $g_{1in,1out}$.

Since we have two RG-relevant boundary operator couplings which affect the transmission conductance across the constriction in opposite ways, we need to determine the conditions under which one wins over the other. From the scaling dimensions of the two operators (as employed in their respective RG equations), we can see that the two couplings grow equally fast for a critical ν_2^* ,

$$\nu_2^* = \frac{\nu_1}{1 + \nu_1}. \quad (45)$$

For this critical ν_2^* , then, the transmission and reflection conductances will be held fixed by the generalized quasiparticle-quasihole symmetry all along the RG flow from weak to strong coupling. For $\nu_2 < \nu_2^*$, λ_1 dominates over λ_2 , which will lead to a minimum of the transmission conductance (i.e., a maximum in the reflection conductance) at low energies (bias or temperature) given by the bulk conductance ν_1 . The quantum Hall constriction system will then resemble that of two quantum Hall droplets separated by vacuum, shown in Fig. 7. Similarly, for $\nu_2 > \nu_2^*$, λ_2 dominates over λ_1 and will lead to the opposite case of a maximum in the transmission conductance (i.e., a minimum in the reflection conductance) at low energies (bias or temperature) given by the bulk conductance ν_1 . The quantum Hall constriction system will then resemble that of a single quantum Hall bar, shown in Fig. 6. As was discussed in detail in an earlier section, these were, indeed, many of the puzzling experimental findings of Refs. 6–8.

We can see that, for the critical value of ν_2^* predicted by our theory, the symmetry-determined (i.e., energy scale independent) constriction transmission conductance is given by

$$t(\nu_2^*) = \frac{g_{1in,1out}(\nu_2^*)}{G_b} = \frac{\nu_2^*}{\nu_1} = \frac{1}{1 + \nu_1} = 1 - \nu_2^*. \quad (46)$$

We now present the above results for the first three generations of the hierarchical sequence of quantum Hall states.

(i) For the bulk filling factor belonging to the primary sequence $\nu_1 = 1/(2p-1)$, we obtain

$$\nu_2^* = \frac{1}{2p}, \quad t(\nu_2^*) = \frac{2p-1}{2p}. \quad (47)$$

Specifically, for $\nu_1 = 1$, we get $\nu_2^* = 1/2 = t(\nu_2^*)$ and, for $\nu_1 = 1/3$, we get $\nu_2^* = 1/4$ and $t(\nu_2^*) = 3/4$. Both these sets of results match the experimental findings of Refs. 6–8.

(ii) Further, we find that for the case of the second generation of the hierarchical states, $\nu_1 = 2p/(2pq \pm 1)$ (where $p=1, q=3, 5, \dots$), we find

$$\nu_2^* = \frac{2p}{2p(1+q) \pm 1}, \quad t(\nu_2^*) = \frac{2pq \pm 1}{2p(1+q) \pm 1}. \quad (48)$$

Specifically, for the case of $\nu_1 = 2/5$, $\nu_2^* = 2/7$ and $t(\nu_2^*) = 5/7$.

(iii) Extending these results to the third generation of the hierarchical states, $\nu_1 = 4p_1 p_2 / [q(4p_1 p_2 \pm 1) \pm 2p_2]$ (where $p_1 = 1 = p_2, q = 3, 5, \dots$), we obtain

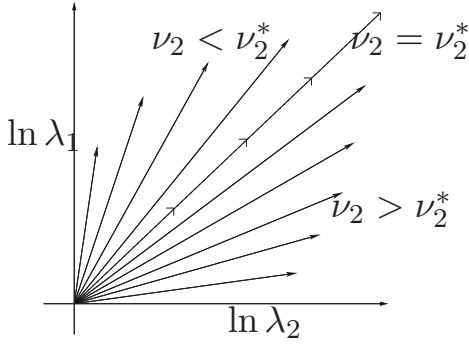


FIG. 9. The RG phase diagram for the model as a plot of the function $\ln \lambda_1 / \ln \lambda_2 = \nu_1(1/\nu_2 - 1)$. All RG flows lead away from the weak-coupling unstable fixed point at the origin. Properties of the dashed critical line and regions above ($\nu_2 < \nu_2^*$) and below ($\nu_2 > \nu_2^*$) are explained in the text.

$$\nu_2^* = \frac{4p_1p_2 \pm 1}{[(1+q)(4p_1p_2 \pm 1) \pm 2p_2]},$$

$$t(\nu_2^*) = \frac{q(4p_1p_2 \pm 1) \pm 2p_2}{(1+q)(4p_1p_2 \pm 1) \pm 2p_2}. \quad (49)$$

Specifically, for the case of $\nu_1 = 3/7$, $\nu_2^* = 3/10$ and $t(\nu_2^*) = 7/10$. The results presented for the cases of $\nu_1 = 2/5$ and $3/7$ can be tested experimentally, and we will comment on this in a later section.

Finally, we present the RG phase diagram of the model in Fig. 9. The origin represents the family of weak-coupling fixed point theories at partial transmission described earlier, while the RG flows are to the familiar fixed point theories^{11,17} of complete reflection ($\nu_2 < \nu_2^*$, see Fig. 7), complete transmission ($\nu_2 > \nu_2^*$, see Fig. 6), and to a different symmetry dictated fixed point theory on the diagonal ($\nu_2 = \nu_2^*$). The diagonal is, in fact, a separatrix—a line of gapless critical theories all possessing the quasiparticle-quasihole symmetry described above—dividing RG flows to a metallic phase (as evidenced by the perfect transmission through the constriction) and an insulating phase (as seen by the perfect reflection at the constriction) at strong coupling. The quasiparticle-quasihole symmetry of the constriction system can also be seen in the reflection symmetry of the RG flows in the two segments on either side of the separatrix: in physical terms, this means that while the upper (lower) segment represents RG flows toward a quasiparticle insulator (metal), the picture is exactly reversed for a description in terms of quasiholes. This is also amply clear in terms of the comparison of the two scaling dimensions: this analysis answers the question as to which of the quasiparticle and quasihole boundary degrees of freedom (given above in the two boundary theories for quasiparticle and quasihole tunneling, respectively) becomes massive first, thereby allowing the remaining gapless boundary degrees of freedom to determine the low-energy, long-wavelength dynamics of the quantum Hall constriction system at strong coupling. Finally, this symmetry of the RG phase diagram is reminiscent of the edge-state transmission duality^{39,40} that is known to exist in

the Chalker-Coddington model⁴¹ as applied to the study of the quantum Hall transitions.

The interesting structure of the RG phase diagram, thus, reflects on the fact that the experimentally observed gate-voltage tuned metal-insulator transition (at vanishing edge bias) is, in fact, shaped not only by boundary critical phenomena (i.e., local interedge quasiparticle tunneling processes, relying on an interplay of the physics of impurity scattering and electron-electron interactions¹¹), but also by the presence of a global symmetry (i.e., the quasiparticle-quasihole conjugation symmetry) and the requirement of overall current conservation in the system. These findings highlight the remarkable generalization of the quantum impurity problem of Refs. 11 and 17 that has been accomplished here. We can now proceed to a study of the correlators and conductances of the system in the next section, with an effort toward reinforcing the physical picture presented by these RG flows.

V. CORRELATORS AND CONDUCTANCES OF THE CONSTRICTION MODEL

In this section, we present computations of various density-density correlators of the fields in the constriction model for the three cases of weak-coupling ballistic transport (i.e., no interedge tunneling), strong coupling with interedge tunneling for $\nu_2 < \nu_2^*$, and strong coupling with interedge tunneling for $\nu_2 > \nu_2^*$. We then employ these correlators in a Kubo formulation to compute the chiral linear dc conductances of the system. In this way, we will confirm the physical picture of the dip-to-peak evolution developed in the last section. We will, in this way, also be able to see the consequence of the quasiparticle-quasihole symmetry on measurable quantities like conductances, confirming the physical picture of transport through the constriction system presented earlier.

In all that follows, we switch from the Euclidean time τ to Matsubara frequencies $\bar{\omega}_n$. This will also be seen to facilitate the computation of the linear dc conductances. Thus, we begin by computing certain density-density correlators, e.g., $\langle [\partial_x \phi_{\bar{\omega}_n}^{1in}(x), \partial_x \phi_{-\bar{\omega}_n}^{1out}(x')] \rangle$, for the free theory S given earlier (i.e., S in the absence of all interedge tunneling processes)

$$\begin{aligned} & \langle [\partial_x \phi_{\bar{\omega}_n}^{1in}(x), \partial_x \phi_{-\bar{\omega}_n}^{1out}(x')] \rangle \\ &= \langle [(\partial_x \phi_{-a}^u + \partial_y \phi_{-a}^l)(\partial_x \phi_a^u + \partial_y \phi_{-a}^r)] \rangle e^{-|\bar{\omega}_n(x'-x-2a)/v|} \\ &= \langle [\partial_x \phi_{-a}^u, \partial_x \phi_{-a}^u] \rangle e^{-|\bar{\omega}_n(x'-x)/v|} \\ &= \frac{2\pi\nu_2}{v^2} |\bar{\omega}_n| e^{-|\bar{\omega}_n(x'-x)/v|}, \end{aligned} \quad (50)$$

where we have used the commutation relations for the various fields and the fact that all transport on the various edges are ballistic and described by the solutions to the chiral equations of motion for the edge density waves given earlier. Further, for the sake of notational brevity, we suppressed the $\bar{\omega}_n$ frequencies in all subscripts on the right hand side, keeping only the spatial dependence in the subscripts in the correlator expressions. The $e^{-|\bar{\omega}_n(x'-x)/v|}$ factor is the expected

phase (easily seen upon performing an analytic continuation to real frequencies ω) associated with the ballistic transport between the points x and x' . As we will soon see when deriving the expressions for the linear dc conductances, this phase factor vanishes upon taking the limit of vanishing frequencies, while the filling factor dependence is crucial.

In the same way, we find the other density-density correlators between the fields outside the constriction as

$$\begin{aligned} \langle [\partial_x \phi_{\bar{\omega}_n}^{1in}(x), \partial_x \phi_{-\bar{\omega}_n}^{2out}(x')] \rangle &= -\frac{2\pi(\nu_1 - \nu_2)}{v^2} |\bar{\omega}_n| e^{-|\bar{\omega}_n(x'-x)/v|}, \\ \langle [\partial_x \phi_{\bar{\omega}_n}^{2in}(x), \partial_x \phi_{-\bar{\omega}_n}^{2out}(x')] \rangle &= -\frac{2\pi\nu_2}{v^2} |\bar{\omega}_n| e^{-|\bar{\omega}_n(x'-x)/v|}, \\ \langle [\partial_x \phi_{\bar{\omega}_n}^{2in}(x), \partial_x \phi_{-\bar{\omega}_n}^{1out}(x')] \rangle &= \frac{2\pi(\nu_1 - \nu_2)}{v^2} |\bar{\omega}_n| e^{-|\bar{\omega}_n(x'-x)/v|}. \end{aligned} \quad (51)$$

We now turn to the case of strong-coupling interedge tunneling within the constriction. Here, three scenarios can be realized, and we study each of them in turn. First, for the case of $\nu_2 < \nu_2^*$, we have already seen that quasiparticle tunneling between the upper and lower edges of the constriction region dominates at strong coupling. Then, from the boundary theory given earlier, it is clear that this strong-coupling scenario possesses another boundary condition (dynamically generated due to the RG flow): $\phi''(x=0) = \phi'(x=0)$. Using this boundary condition while computing the four density-density correlators given above, we find

$$\begin{aligned} \langle [\partial_x \phi_{\bar{\omega}_n}^{1in}(x), \partial_x \phi_{-\bar{\omega}_n}^{1out}(x')] \rangle &= 0, \\ \langle [\partial_x \phi_{\bar{\omega}_n}^{1in}(x), \partial_x \phi_{-\bar{\omega}_n}^{2out}(x')] \rangle &= -\frac{2\pi\nu_1}{v^2} |\bar{\omega}_n| e^{-|\bar{\omega}_n(x'-x)/v|}, \\ \langle [\partial_x \phi_{\bar{\omega}_n}^{2in}(x), \partial_x \phi_{-\bar{\omega}_n}^{2out}(x')] \rangle &= 0, \\ \langle [\partial_x \phi_{\bar{\omega}_n}^{2in}(x), \partial_x \phi_{-\bar{\omega}_n}^{1out}(x')] \rangle &= \frac{2\pi\nu_1}{v^2} |\bar{\omega}_n| e^{-|\bar{\omega}_n(x'-x)/v|}. \end{aligned} \quad (52)$$

It is easy to see from these correlators that the physical system here is that visualized in Fig. 7.

Next, for the case of $\nu_2 > \nu_2^*$, we have already determined that quasiparticle tunneling between the left and right edges of the constriction region dominates at strong coupling. Then, from the boundary theory given earlier, it is clear that this strong-coupling scenario possesses another boundary condition (again, dynamically generated due to the RG flow): $\phi'(y=0) = \phi''(y=0)$. Using this boundary condition while computing the four density-density correlators given above, we find

$$\begin{aligned} \langle [\partial_x \phi_{\bar{\omega}_n}^{1in}(x), \partial_x \phi_{-\bar{\omega}_n}^{1out}(x')] \rangle &= \frac{2\pi\nu_1}{v^2} |\bar{\omega}_n| e^{-|\bar{\omega}_n(x'-x)/v|}, \\ \langle [\partial_x \phi_{\bar{\omega}_n}^{1in}(x), \partial_x \phi_{-\bar{\omega}_n}^{2out}(x')] \rangle &= 0, \end{aligned}$$

$$\langle [\partial_x \phi_{\bar{\omega}_n}^{2in}(x), \partial_x \phi_{-\bar{\omega}_n}^{2out}(x')] \rangle = -\frac{2\pi\nu_1}{v^2} |\bar{\omega}_n| e^{-|\bar{\omega}_n(x'-x)/v|},$$

$$\langle [\partial_x \phi_{\bar{\omega}_n}^{2in}(x), \partial_x \phi_{-\bar{\omega}_n}^{1out}(x')] \rangle = 0. \quad (53)$$

It is again easy to see from these correlators that the physical system here is that visualized in Fig. 6.

Finally, we turn to considering the quasiparticle-quasihole symmetric case of $\nu_2 = \nu_2^*$. It is clear that since the two RG flows to strong coupling indicate opposing tendencies on the system, i.e., very different physical configurations for the system (Figs. 6 and 7, respectively), the equally fast growth of both couplings still cannot lead to the generation of any new boundary conditions in this case. It is then easily concluded that all the density-density correlators studied above must appear to be exactly the same at strong coupling as found to be at weak coupling (and, indeed, all along the RG flow). Thus, the consequence of the global symmetry of quasiparticle-quasihole conjugation is to keep the various transmission and reflection edge fields at the constriction from becoming massive locally. This confirms the existence of a line of critical (gapless) theories, all possessing the symmetry mentioned above and unstable to relevant RG perturbations upon changing the parameter ν_2 from its critical value; the correlators confirm that the RG flow is toward strong-coupling theories, where either the transmitting or the reflecting edges become massive locally, suppressing some of the correlators while giving the other correlators the values they would have in the two scenarios in Figs. 6 and 7.

As we will now see, by using the fact that the charge and current densities for a chiral edge bosonic field ϕ are simply related to another, these density-density correlators can be employed in computing several two-terminal chiral linear (dc) conductances. These conductances can be derived from a linear response type Kubo formulation,^{11,14,42} yielding relations linking them to the correlators computed above in the form of retarded response functions (obtained upon performing an analytic continuation from Matsubara frequencies $\bar{\omega}_n$ to real frequencies ω)

$$g_{\alpha\beta}(x, x') = \lim_{\omega \rightarrow 0} (-1)^{[\tilde{\alpha} + \tilde{\beta}]} \frac{e^2 v^2}{2\pi\hbar\omega} \langle [\partial_x \phi_{\omega}^{\alpha}(x), \partial_x \phi_{-\omega}^{\beta}(x')] \rangle, \quad (54)$$

where $(\alpha, \beta) = (1in, \dots, 2out)$ are the terminal indices, $(\tilde{\alpha}, \tilde{\beta})$ are the terminal numbers (i.e., 1 and 2) associated with these terminal indices, and $[\tilde{\alpha} + \tilde{\beta}]$ is a number modulo 2 such that the factor $(-1)^{[\tilde{\alpha} + \tilde{\beta}]}$ restores the direction of net current flow from source to drain as positive. From the expressions for the correlators given earlier, it is clear that in the dc limit $\omega \rightarrow 0$, the linear conductances no longer depend on the spatial coordinates of x and x' ; this is a consequence of the fact that transport along the edges is ballistic and equilibration takes place only in the reservoirs.⁴² We can now simply use the various correlators computed above in calculating the various two-terminal chiral linear conductances of the system. For the sake of brevity, we summarize in Table I our calculations of the chiral linear conductances $g_{1in,1out}$ and $g_{1in,2out}$

TABLE I. Values of two chiral linear conductances, $g_{1in,1out}$ and $g_{1in,2out}$, representing the transmission and reflection through the constriction at weak coupling (ballistic transport only) and the three strong-coupling scenarios of $\nu_2 < \nu_2^*$, $\nu_2 > \nu_2^*$, and $\nu_2 = \nu_2^*$.

| Constriction filling ν_2 | $g_{1in,1out}$ (e^2/h) | $g_{1in,2out}$ (e^2/h) |
|--|-------------------------------|-------------------------------|
| Weak coupling | ν_2 | $\nu_1 - \nu_2$ |
| Strong coupling ($\nu_2 < \nu_2^*$) | 0 | ν_1 |
| Strong coupling ($\nu_2 > \nu_2^*$) | ν_1 | 0 |
| Strong coupling ($\nu_2 = \nu_2^*$) | ν_2 | $\nu_1 - \nu_2$ |

representing the transmission and reflection through the constriction, at weak coupling (ballistic transport only) and the three strong coupling scenarios of $\nu_2 < \nu_2^*$, $\nu_2 > \nu_2^*$, and $\nu_2 = \nu_2^*$.

The other two conductances $g_{2in,1out}$ and $g_{2in,2out}$ can be computed in precisely the same manner. The physical picture of weak-coupling ballistic transport and the three strong-coupling scenarios presented earlier is immediately confirmed from the expressions given in Table I. The finite temperature T (or voltage V) expressions for the perturbative corrections to the weak-coupling ballistic chiral conductances due to the quasiparticle and quasihole interedge tunneling processes revealed earlier can also be computed from the boundary theories presented earlier.¹¹ Thus, we find that

$$\begin{aligned} \delta g_{1in,1out}^{WC} &= g_{1in,1out} - \nu_2 \frac{e^2}{h} = -c_1 \frac{e^2}{h} \lambda_1^2 T^{2\nu_2-2} + c_2 \frac{e^2}{h} \lambda_2^2 T^{-2\nu_2/\nu_1}, \\ \delta g_{1in,2out}^{WC} &= g_{1in,2out} - (\nu_1 - \nu_2) \frac{e^2}{h} \\ &= +c_3 \frac{e^2}{h} \lambda_1^2 T^{2\nu_2-2} - c_4 \frac{e^2}{h} \lambda_2^2 T^{-2\nu_2/\nu_1}, \end{aligned} \quad (55)$$

where (c_1, \dots, c_4) are nonuniversal constants. We conclude by noting that, for the quasiparticle-quasihole symmetric critical constriction filling factor of ν_2^* , the tunneling strengths $\lambda_1 \equiv \lambda_2$, while the constants are related as $c_1 = c_2$ and $c_3 = c_4$, such that the corrections to the chiral linear conductances given above vanish, $\delta g_{1in,1out}^{WC, \nu_2^*} = 0 = \delta g_{1in,2out}^{WC, \nu_2^*}$. This provides a more quantitative explanation of the edge-bias-independent constriction transmission observed experimentally.⁶

VI. COMPARISON WITH THE EXPERIMENTS

In this section, we bring together all our results in order to compare them with the findings of the experiments.^{6-8,10} In our phenomenological model for edge-state transport in the presence of a gate-voltage controlled constriction, we have chosen to model the constriction by a mesoscopic region of lowered electronic density (and, hence, filling fraction ν_2) in

comparison to that in the bulk (of filling fraction ν_1). The reduced transmission through the constriction at high edge bias (i.e., partial transmission ballistic transport) is explained in terms of the transmitting edge states of the constriction, whose properties are governed solely by the constriction quantum Hall fluid. Further, the experimentally observed current backscattered from the constriction (and received in a terminal on the opposite side of the Hall bar) is explained in terms of the existence of a gapless edge state lying in between the bulk and constriction quantum Hall fluids (and whose properties are governed by both the bulk as well as the constriction fluids).

Next, the startling dip-to-peak evolution of the vanishing bias constriction transmission with decreasing strength of the gate voltage is understood as the result of a competition between local interedge quasiparticle (quasihole) tunneling events among the transmitting (reflecting) edges of the constriction region. The edge-bias-independent constriction transmission is seen to arise from the quasiparticle-quasihole symmetric critical theories that lie on the separatrix of the RG phase diagram; the equal and opposite growth of the two interedge tunneling processes leads to an exact cancellation of any gap generating processes. These critical theories are characterized by a critical value of $\nu_2 = \nu_2^*$ and separate relevant RG flows to either of the cases of perfect or zero transmission through the constriction. The values of the critical ν_2^* and the constriction transmission at this value, $t(\nu_2^*)$, are seen to match exactly those obtained experimentally for the cases of the bulk $\nu_1 = 1$ and $1/3$.^{6,7} Further, the experimental finding of $t(\nu_2^*)$ lying between 0.7 and 0.8 for both the cases of $\nu_1 = 2/5$ and $\nu_1 = 3/7$ (Ref. 8) appear to be consistent with those obtained from the results from our model. More rigorous experimental investigations of the $\nu_1 = 2/5$ and $3/7$ systems may, however, be necessary to make a firmer statement. Further, the two dip-to-peak evolutions observed for the case of $\nu_1 = 2$ (Ref. 6) is easily understood from our model as long as we assume zero inter-Landau-level mixing. Finally, the phenomenological assumptions of (i) a constriction region characterized simply by one parameter, ν_2 , and (ii) only local interedge tunneling events inside the constriction appear to be robust against changes in the size and shape of the constriction (i.e., the size and shape of the gate-voltage plates which create the constriction through electrostatic means); this is consistent with the experimental results of Ref. 10.

We now evaluate the relevance of our model in understanding the findings of a recent work on a constriction circuit with the bulk at $\nu_1 = 3$.⁴³ In this work, the authors appear to find evidence for a zero-bias resistance peak for the case of the constriction at $\nu_2 = 5/2$. Levin *et al.*, in a very recent work,⁴⁴ attributed this to the possibility of a Pfaffian (Pf) $5/2$ state existing in the constriction quantum Hall fluid, rather than its particle-hole conjugate anti-Pfaffian state. For this, they appear to use the simple model for the constriction first revealed in Ref. 27 (and further elaborated upon here), together with the fact that they find the interedge tunnel coupling between the transmitting edges (λ_1 in our work) to be more RG relevant than the interedge tunnel coupling between the reflecting edges (λ_2 in our work). Thus, this experimental observation⁴³ appears, at first sight, to be inconsistent with our results for the case of $\nu_1 = 3$: specifically, our

analysis predicts that the constriction filling fraction of $\nu_2 = 5/2$ is critical, and the constriction transmission should, therefore, be edge-bias independent [as observed in the experiments for the cases of $\nu_2 = 1/2$, $\nu_1 = 1$ and $\nu_2 = 3/2$, $\nu_1 = 2$ (Ref. 6)]. While Miller *et al.*⁴³ found a zero-bias resistance peak at $\nu_2 = 7/3$ in consistency with the predictions from our analysis, experimental results at $\nu_2 = 8/3$ (where our analysis predicts the existence of a zero-bias resistance minimum) are as yet forthcoming.

A closer look, however, reveals that the inconsistency for the case of $\nu_2 = 5/2$ arises from the following fact. The analysis of the quantum Hall constriction system carried out in the present work relies on the assumption that the quantum Hall ground states in the bulk as well as constriction regions are completely spin polarized, have only two-body interactions, exactly $1/2$ electron per magnetic flux, and no inter-Landau-level mixing. The Pf state, on the other hand, is the exact ground state of a three-body interaction which explicitly breaks particle-hole symmetry.⁴⁵ It is, therefore, not surprising that the predictions of edge-state theories based on these two bulk quantum Hall states should be quite different. This is seen, for instance, in the existence of neutral Majorana fermion edge modes for the case of the non-Abelian Pf $5/2$ ground state, while our model presently addresses only the charge carrying edge modes for an Abelian quantum Hall ground state. Most notably, the interedge quasiparticle tunneling exponents in the two cases will be different. A more systematic experimental study of the $\nu_1 = 3$ constriction system along the lines of that conducted by Roddaro *et al.* for the $\nu_1 = 1$ system⁶ could, therefore, improve considerably our understanding of the nature of the $\nu = 5/2$ quantum Hall ground state.

VII. SUMMARY AND OUTLOOK

In this work, we have introduced a model which describes intermediate conductance scenarios in the problem of tunneling in 1D chiral systems by constructing a model for a constricted region (i.e., with a lower filling fraction, ν_2 , than that of the Hall fluid in the bulk, ν_1). A Landauer-Buttiker analysis of ballistic transport reveals that the constriction acts as a junction for the chiral density waves incident on it by splitting them into currents on the transmitting and reflecting arms of the constriction region. An edge-state model is then formulated in terms of a hydrodynamic theory of long-wavelength, low-energy chiral density-wave excitations. Specifically, we are able to describe the dynamics of the constriction junction in terms of two pairs of edge fields, (ϕ^u, ϕ^d) and (ϕ^l, ϕ^r) , whose properties are governed by the effective filling fractions ν_2 and $\nu_1 - \nu_2$, respectively. The constriction is connected to two incoming- and two outgoing-chiral modes. Introducing local quasiparticle tunneling across various arm pairs of the constriction, we derive the perturbative RG equations for the various tunnel couplings and find that the RG flow is toward strong coupling for both the tunnel couplings considered. A competition between the two couplings to reach the strong-coupling regime determines the low-energy configuration of the system. A quasiparticle-quasihole symmetry of the system is found to

determine the existence of a line of critical (gapless) theories at a critical filling fraction of the constriction region (ν_2^*) which separates the relevant RG flows toward the perfect transmission and reflection strong-coupling fixed point theories. The conductances $g_{1in,1out}$ and $g_{1in,2out}$ are computed in the weak- and strong-quasiparticle tunneling coupling limits and are also found to match qualitatively the experimental findings of Refs. 6 and 7. We are also able to recover the familiar results for $\nu_2 = \nu_1$.^{11,14} In this way, we have achieved a nontrivial generalization of the generic phenomenological model of tunneling in FQHE systems formulated by Kane and co-workers.^{11,14}

Given the success the phenomenological edge model proposed in this work meets in providing explanations for the various puzzling experimental observations, we now turn to a discussion of certain aspects of the model. First, the model relies essentially on treating the filling fractions of the quantum Hall ground state in the bulk (ν_1) and constriction (ν_2) regions as the two parameters of the model. While such a model is sensible for the case of when both (ν_1, ν_2) take values from among the special fractions representing incompressible quantum Hall ground states, how far can we trust it for the case of when the quantum Hall ground states in the bulk and constriction regions are compressible? The answer could lie in a work by Levitov *et al.*⁴⁶ that provides a generalization of the chiral TLL edge state to the case of a compressible quantum Hall state in the bulk via a composite-fermion Chern-Simons formulation. Thus, it should be possible to derive the edge model for the constriction system proposed here for a general quantum Hall ground state by proceeding along similar lines.

Further, the multimode nature of the edge state of several members of the incompressible Jain hierarchy of quantum Hall states, involving one charged edge mode and several charge neutral modes, is a well established fact theoretically. Thus, it is worth understanding how the present model (with its assumption of a single edge mode everywhere in the circuit) fares so well in its comparison with the experiments even in describing such quantum Hall states. A possible microscopic explanation can be found by assuming that the velocity of the charge mode is much greater than those of the various neutral modes of a multimode edge state.⁴⁷ Under such circumstances, the dynamics of only the charge edge mode becomes important in an intermediate energy regime, while the responses arising from the various neutral modes can be ignored. Further, the composite-fermion field theoretic formulation by Lopez and Fradkin departs from the multimode picture of the QH edge for the incompressible Jain fractions;⁴⁸ this construction involves only one charge mode (and two auxiliary Klein factors which do not have any additional propagating degrees of freedom). In this sense, this formulation can be likened to the other multimode edge theories with vanishing neutral mode velocities. Finally, for the case of integer quantum Hall systems, it is worth noting that recent numerical works by Siddiki and co-workers⁴⁹ suggest that quantum Hall systems at higher (integer) ν filling fractions generically involve only one edge mode in charge transport.

The present work can clearly be generalized to the case of more than four chiral wires meeting at a junction. This is

important in modeling the transport across various kinds of junctions of several nonchiral Tomonaga-Luttinger liquid wires, where the RG phase diagram is known to contain several nontrivial fixed points.⁵⁰⁻⁵⁵ Studies of resonant-tunneling junctions (i.e., junctions which possess a resonant two-level system or spin-1/2 degree of freedom in addition to allowing quasiparticle tunneling^{11,50,53,55}) reveal interesting transport phenomena (including variations of the Kondo and Coulomb-blockade effects); a resonant-tunneling constriction junction is likely to possess novel variations of the phenomena found in these works.

Several experimental studies of noise correlations in quantum Hall edge systems (both the integer^{56,57} and fractional^{8,9} kind), where Hanbury-Brown-Twiss type correlations have been analyzed through current splitters created using split-gated constrictions on quantum Hall samples, have thrown up many interesting results. A similar study has also been performed with a point contact in a 2DEG.⁵⁸ Recently, experimental observations on the interference fringes in the source-drain conductance of a Mach-Zehnder interferometer made out of edge states in the integer quantum Hall system have received a lot of attention.⁵⁹ It would, therefore, be very interesting to study the current-noise correlations of the constriction junction model we have set up in the present work.

This study has also revealed the existence of gapless edge states that lie in between gapped quantum Hall fluids with differing filling factors. In our study, such states carried the reflected current between the two edges of the Hall bar, making the scenario essentially one of intermediate transmission. While the phenomenological hydrodynamic edge-state

model developed in the present work, and containing these edge states, meets with considerable success in explaining the various puzzles presented by the experiments,^{6,8} it will be even more satisfying to explore the emergence of such a model from that of a theory containing the bulk degrees of freedom as well. Such an investigation can be carried out by starting from a Chern-Simons Ginzburg-Landau type theory⁶⁰ of a quantum Hall with a spatially dependent filling factor, and which will be the focus of a future work. Finally, we note that it remains a challenge to be able to develop a microscopic understanding of the dependence of the constriction filling fraction ν_2 proposed in our model on the gate voltage V_g . Accomplishing this will allow us to make detailed quantitative comparisons with available experimental data as well as propose future experiments.

ACKNOWLEDGMENTS

I am grateful to D. Sen and S. Rao for many stimulating discussions and constant encouragement. I would like to thank A. Altland, B. Rosenow, and Y. Gefen for many invaluable discussions on various aspects of quantum Hall edge state transport as well as S. Roddaro, V. Pellegrini, and M. Heiblum in helping my understanding of their experiments. Special thanks are also due to S. Vishveshwara, M. Stone, G. Murthy, A. Siddiki, R. Mazzarello, F. Franchini, I. Safi, F. Dolcini, and A. Nersesyan for discussions on quantum Hall physics. I am indebted to the Centre for Condensed Matter Theory, Indian Institute of Science, Bangalore, and the Harishchandra Research Institute, Allahabad, for their hospitality while this work was carried out.

*slal@ictp.it

¹Thierry Giamarchi, *Quantum Physics in One Dimension* (Oxford University Press, Oxford, 2004), and references therein.
²X. G. Wen, Phys. Rev. B **41**, 12838 (1990); **43**, 11025 (1991); **44**, 5708 (1991).
³X. G. Wen, Int. J. Mod. Phys. B **6**, 1711 (1992).
⁴A. M. Chang, Rev. Mod. Phys. **75**, 1449 (2003).
⁵X. G. Wen, Adv. Phys. **44**, 405 (1995).
⁶S. Roddaro, V. Pellegrini, F. Beltram, L. N. Pfeiffer, and K. W. West, Phys. Rev. Lett. **95**, 156804 (2005).
⁷S. Roddaro, V. Pellegrini, F. Beltram, G. Biasiol, and L. Sorba, Phys. Rev. Lett. **93**, 046801 (2004).
⁸Y. C. Chung, M. Heiblum, and V. Umansky, Phys. Rev. Lett. **91**, 216804 (2003).
⁹E. Comferti, Y. C. Chung, M. Heiblum, V. Umansky, and D. Mahalu, Nature (London) **416**, 515 (2002).
¹⁰S. Roddaro, U. Perinetti, V. Pellegrini, F. Beltram, L. N. Pfeiffer, and K. W. West, Physica E (Amsterdam) **34**, 132 (2006).
¹¹C. L. Kane and M. P. A. Fisher, Phys. Rev. Lett. **68**, 1220 (1992); Phys. Rev. B **46**, 15233 (1992).
¹²See M. P. A. Fisher and L. I. Glazman, in *Mesoscopic Electron Transport*, edited by L. Kouwenhoven, G. Schön, and L. Sohn, NATO Advanced Studies Institute, Series E: Applied Science

(Kluwer Academic, Dordrecht, 1997), Vol. 345 for an excellent review.

¹³A. O. Gogolin, A. A. Nersesyan, and A. M. Tsvelik, *Bosonization and Strongly Correlated Systems* (Cambridge University Press, Cambridge, England, 1998).
¹⁴K. Moon, H. Yi, C. L. Kane, S. M. Girvin, and M. P. A. Fisher, Phys. Rev. Lett. **71**, 4381 (1993).
¹⁵A. Furusaki and N. Nagaosa, Phys. Rev. B **47**, 4631 (1993).
¹⁶E. Wong and I. Affleck, Nucl. Phys. B **417**, 403 (1994).
¹⁷P. Fendley, A. W. W. Ludwig, and H. Saleur, Phys. Rev. Lett. **74**, 3005 (1995); Phys. Rev. B **52**, 8934 (1995).
¹⁸Y. Oreg and A. M. Finkel'stein, Phys. Rev. Lett. **74**, 3668 (1995).
¹⁹L. P. Pryadko, E. Shimshoni, and A. Auerbach, Phys. Rev. B **61**, 10929 (2000).
²⁰V. M. Apalkov and M. E. Raikh, Phys. Rev. B **68**, 195312 (2003).
²¹C. L. Kane and M. P. A. Fisher, Phys. Rev. B **51**, 13449 (1995).
²²D. B. Chklovskii and B. I. Halperin, Phys. Rev. B **57**, 3781 (1998); N. P. Sandler, C. C. Chamon, and E. Fradkin, *ibid.* **57**, 12324 (1998).
²³C. C. Chamon and E. Fradkin, Phys. Rev. B **56**, 2012 (1997).
²⁴J. E. Moore, P. Sharma, and C. Chamon, Phys. Rev. B **62**, 7298 (2000).
²⁵J. E. Moore and X. G. Wen, Phys. Rev. B **66**, 115305 (2002).
²⁶D. Giuliano and P. Sodano, Nucl. Phys. B **770**, 332 (2007).

- ²⁷S. Lal, *Europhys. Lett.* **80**, 17003 (2007).
- ²⁸E. Papa and T. Stroh, *Phys. Rev. Lett.* **97**, 046801 (2006); *Phys. Rev. B* **75**, 045342 (2007).
- ²⁹E. Papa and A. H. MacDonald, *Phys. Rev. Lett.* **93**, 126801 (2004); *Phys. Rev. B* **72**, 045324 (2005).
- ³⁰R. D'Agosta, R. Raimondi, and G. Vignale, *Phys. Rev. B* **68**, 035314 (2003); L. P. Pryadko, E. Shimshoni, and A. Auerbach, *ibid.* **61**, 10929 (2000).
- ³¹M. Büttiker, Y. Imry, R. Landauer, and S. Pinhas, *Phys. Rev. B* **31**, 6207 (1985); S. Datta, *Electronic Transport in Mesoscopic Systems* (Cambridge University Press, Cambridge, England, 1995); *Transport Phenomenon in Mesoscopic Systems*, edited by H. Fukuyama and T. Ando (Springer Verlag, Berlin, 1992); Y. Imry, *Introduction to Mesoscopic Physics* (Oxford University Press, New York, 1997).
- ³²S. Komiyama, H. Hirai, S. Sasa, and S. Hiyamizu, *Phys. Rev. B* **40**, 12566 (1989).
- ³³M. Büttiker, *Phys. Rev. Lett.* **57**, 1761 (1986); *IBM J. Res. Dev.* **32**, 317 (1988).
- ³⁴V. V. Ponomarenko and D. V. Averin, *Phys. Rev. B* **67**, 035314 (2003); **70**, 195316 (2004).
- ³⁵A. H. Castro Neto, C. deC. Chamon, and C. Nayak, *Phys. Rev. Lett.* **79**, 4629 (1997).
- ³⁶D. Yoshioka, *The Quantum Hall Effect*, Springer Series in Solid-State Sciences Vol. 133 (Springer, Berlin, 2002), and references therein.
- ³⁷S. Lal, S. Rao, and D. Sen, *Phys. Rev. Lett.* **87**, 026801 (2001); *Phys. Rev. B* **65**, 195304 (2001).
- ³⁸S. M. Girvin, *Phys. Rev. B* **29**, 6012 (1984).
- ³⁹E. Shimshoni, S. L. Sondhi, and D. Shahar, *Phys. Rev. B* **55**, 13730 (1997).
- ⁴⁰S. Xiong, *Phys. Rev. B* **57**, 9928 (1998).
- ⁴¹J. T. Chalker and P. D. Coddington, *J. Phys. C* **21**, 2665 (1988).
- ⁴²C. L. Kane and M. P. A. Fisher, in *Perspectives in Quantum Hall Effects*, edited by S. Das Sarma and A. Pinczuk (Wiley, New York, 1997).
- ⁴³J. B. Miller, I. P. Radu, D. M. Zumbühl, E. M. Levenson-Falk, M. A. Kastner, C. M. Marcus, L. N. Pfeiffer, and K. W. West, *Nat. Phys.* **3**, 561 (2007).
- ⁴⁴M. Levin, B. I. Halperin, and B. Rosenow, *Phys. Rev. Lett.* **99**, 236806 (2007); S.-S. Lee, S. Ryu, C. Nayak, and M. P. A. Fisher, *Phys. Rev. Lett.* **99**, 236807 (2007).
- ⁴⁵M. Greiter, X. G. Wen, and F. Wilczek, *Phys. Rev. Lett.* **66**, 3205 (1991).
- ⁴⁶L. S. Levitov, A. V. Shytov, and B. I. Halperin, *Phys. Rev. B* **64**, 075322 (2001).
- ⁴⁷D. H. Lee and X. G. Wen, arXiv:cond-mat/9809160 (unpublished).
- ⁴⁸A. Lopez and E. Fradkin, *Phys. Rev. B* **59**, 15323 (1999).
- ⁴⁹A. Siddiki and R. R. Gerhardt, *Phys. Rev. B* **70**, 195335 (2004); A. Siddiki and F. Marquardt, *ibid.* **75**, 045325 (2007).
- ⁵⁰C. Nayak, M. P. A. Fisher, A. W. W. Ludwig, and H. H. Lin, *Phys. Rev. B* **59**, 15694 (1999).
- ⁵¹S. Lal, S. Rao, and D. Sen, *Phys. Rev. B* **66**, 165327 (2002).
- ⁵²S. Chen, B. Trauzettel, and R. Egger, *Phys. Rev. Lett.* **89**, 226404 (2002).
- ⁵³C. Chamon, M. Oshikawa, and I. Affleck, *Phys. Rev. Lett.* **91**, 206403 (2003).
- ⁵⁴S. Das, S. Rao, and D. Sen, *Phys. Rev. B* **70**, 085318 (2004).
- ⁵⁵S. Rao and D. Sen, *Phys. Rev. B* **70**, 195115 (2004).
- ⁵⁶M. Henny, S. Oberholzer, C. Strunk, T. Heinzel, K. Ensslin, M. Holland, and C. Shönenberger, *Science* **284**, 296 (1999).
- ⁵⁷S. Oberholzer, M. Henny, C. Strunk, C. Shönenberger, T. Heinzel, K. Ensslin, and M. Holland, *Physica E (Amsterdam)* **6E**, 314 (2000).
- ⁵⁸W. D. Oliver, J. Kim, R. C. Liu, and Y. Yamamoto, *Science* **284**, 299 (1999).
- ⁵⁹Y. Ji, Y. C. Chung, D. Sprinzak, M. Heiblum, D. Mahalu, and H. Shtrikman, *Nature (London)* **422**, 415 (2003); I. Neder, M. Heiblum, Y. Levinson, D. Mahalu, and V. Umansky, *Phys. Rev. Lett.* **96**, 016804 (2006); I. Neder, M. Heiblum, D. Mahalu, and V. Umansky, *ibid.* **98**, 036803 (2007); L. V. Litvin, H.-P. Tranitz, W. Wegscheider, and C. Strunk, *Phys. Rev. B* **75**, 033315 (2007).
- ⁶⁰S. C. Zhang, T. H. Hansson, and S. Kivelson, *Phys. Rev. Lett.* **62**, 82 (1989).